Intralayer-versus-interlayer pairing in the copper oxide superconductors

R. A. Klemm
*Materials Science Division, Argonne National Laboratory, Argonne, Illinois 60439**
and Solid State Division, Oak Ridge National Laboratory, P.O. Box 2008, Oak Ridge, Tennessee 37831-6032

S. H. Liu
Solid State Division, Oak Ridge National Laboratory, P.O. Box 2008, Oak Ridge, Tennessee 37831-6032
(Received 23 August 1990; revised manuscript received 25 April 1991)

We have investigated the competing roles of intralayer s-wave and interlayer BCS-like pairing in determining the c-axis versus ab-plane energy-gap anisotropy in layered superconductors with $N=1,2$ conducting planes per unit-cell edge s. For $N=1$, intralayer s-wave pairing leads to a conventional order parameter (OP) Δ_0 with a transition temperature (T_c) value T_{c0} and isotropic energy gap $2|\Delta_0|$. For interlayer pairing, the four-vector gap function $\tilde{\Delta}_3(k_z)$ contains a singlet OP Δ_s and a vector triplet OP $\mathbf{\Delta}_t$, with corresponding normalized gap functions $\sqrt{2}\cos k_z s$ and $\sqrt{2}\sin k_z s$. Since Δ_s and $\mathbf{\Delta}_t$ have identical T_c values ($T_{cs}=T_{ct}$), the free energy is minimized when $|\Delta_s|=|\mathbf{\Delta}_t|$, and the resulting gap $2|\Delta|$ is found to be *isotropic*. However, $2|\Delta|$ is completely *incompatible* with $2|\Delta_0|$. For $N=2$, there are two intralayer pairing OP's Δ_0 and Δ_1, and two interlayer four-vector gap functions $\tilde{\Delta}_3(k_z)$ and $\tilde{\Delta}_2(k_z)$, all of which could contribute to measurable quantities in the Gaussian-fluctuation regime above the highest T_c value. However, interband pair breaking causes Δ_1 and $\tilde{\Delta}_2$ to vanish below the maximum T_c value. Of the two singlet OP's in $\tilde{\Delta}_3(k_z)$, the OP Δ_s has the higher T_c value, T_{cs}, and the second singlet OP can be neglected. The triplet OP Δ_t has the T_c value $T_{ct}\le T_{cs}$. For $T_{c0}>T_{cs}$, the gap is just $2|\Delta_0|$. For $T_{c0}<T_{ct}$, $\Delta_0=0$ and the gap $2|\Delta(k_z,T)|$ is anisotropic. There are two regions of the parameters with different gap-anisotropy behavior. In region I, the gap is always nodeless, and is nearly pure singlet for weak coupling. In region II, the gap has a pair of nodes near to T_{cs}, but is nodeless at low T, as $|\Delta_t|\neq 0$. For $T_{cs}>T_{c0}>T_{ct}$, the gap $2|\Delta(k_z,T)|$ is anisotropic, nodeless at low T, and could on rare occasions involve $\Delta_0\neq 0$, in addition to $\Delta_s\neq 0$. In any event, the gap is the same on both of the quasiparticle bands. Our results are discussed in terms of recent far-infrared-reflectance, Raman-scattering, and point-contact-tunneling experiments. Additional experiments to clarify the c-axis versus ab-plane gap anisotropy and the microscopic pairing mechanism are suggested.

I. INTRODUCTION

Recently, there have been a number of measurements in various high-transition-temperature (T_c) superconductors that have the potential of giving information regarding the symmetry of the superconducting energy gap 2Δ and the related order parameter(s) (OP's) in those materials. Measurements[1] of the penetration depth $\lambda(T)$ in $YBa_2Cu_3O_{7-\delta}$ (Y 1:2:3) for magnetic fields $\mathbf{H}\|\hat{\mathbf{c}}$ and $\mathbf{H}\perp\hat{\mathbf{c}}$ gave results consistent with BCS behavior in both directions, suggesting that the gap is unlikely to exhibit nodes at low temperatures T in that material, although it could be anisotropic, the possible gap anisotropy being masked by the pair effective-mass anisotropy between the c axis and the ab planes. Magnetization measurements[2] at different azimuthal angles of the critical fields parallel to the ab plane in Y 1:2:3 were consistent with little or no effective-mass anisotropy of the pairs within the ab plane, as well as no nodes of the gap within the ab plane.

Far-infrared-reflectance[3] measurements on twinned crystals of Y 1:2:3 were suggestive of a lack of gap anisotropy within the ab plane, but gave different apparent "gap" values for electric fields $\mathbf{E}\|\hat{\mathbf{c}}$ and $\mathbf{E}\perp\hat{\mathbf{c}}$, suggestive of a gap that is larger within the ab planes than in the $\hat{\mathbf{c}}$ direction. More recent infrared-reflectance measurements[4] on an untwinned single crystal with $\mathbf{E}\|\hat{\mathbf{a}}$ and $\mathbf{E}\|\hat{\mathbf{b}}$ showed the gap to be apparently isotropic within the ab plane, with an apparent $T=0$ magnitude $2\Delta/k_BT_c\sim 8$, consistent with the twinned single-crystal infrared-reflectance results.[3] Similar results suggestive of c axis versus ab-plane gap anisotropy have been obtained[5] by recent Raman-scattering experiments on untwinned single crystals of Y 1:2:3.

Point-contact-tunneling[6,7] measurements on Y 1:2:3 have been interpreted as giving a gap of roughly the same value, but show an additional feature at lower energies that has been interpreted[7] as possibly arising from gap anisotropy, the gap being different for wave vectors $\mathbf{k}\|\hat{\mathbf{c}}$ and $\mathbf{k}\perp\hat{\mathbf{c}}$. Point-contact measurements[8] at positions on the planar surface and on the edges of Y 1:2:3 crystals have also been interpreted as giving evidence for c-axis versus ab-plane gap anisotropy. Recent superconducting-normal-superconducting (SNS') planar tunneling experiments on Y 1:2:3 were reported[9] to exhibit an ac Josephson effect. Other workers found[10] that planar SNS' tunneling into Y 1:2:3 films oriented with the c axis normal to the substrate surface did not give an ac Josephson effect, whereas tunneling into Y 1:2:3 films

with the a axis normal to the substrate did result in the Shapiro steps characteristic of the ac Josephson effect. In addition, NMR experiments on Y 1:2:3 using ^{17}O (Ref. 11) and Cu (Ref. 12) showed no evidence of a Hebel-Slichter peak in the Knight shift, and a Cu Knight shift exhibiting a different T dependence for the Cu ions on the Cu-O chains from those on the Cu-O planes, consistent with c-axis versus ab-plane gas anisotropy. The magnitudes of the low-T Knight shift were found to be inconsistent[12] with purely triplet superconductivity.

A smattering of results for other high-T_c superconductors is also available. Angular resolved photoemission results[13] for $Bi_2Sr_2CaCu_2O_{8+x}$ (Bi 2:2:1:2), in addition to showing a clear Fermi edge on the holelike Cu-O bands (and on the electronlike Bi-O band for one x value studied), are consistent with little, if any, gap anisotropy within the ab planes, the gap appearing to be essentially given by $2\Delta/k_BT_c \sim 8$ at all of the points in reciprocal space investigated to date.[14] The k_z dependence has not yet been investigated[14] by sampling different outgoing energy values at fixed k_x and k_y. Point-contact-tunneling measurements[15] on $La_{2-x}Sr_xCuO_4$ were interpreted as arising from an isotropic gap. In the electron-doped superconductors $Nd_{2-x}Ce_xCuO_4$ and $Nd_{2-x}Th_xCuO_4$, point-contact[16] and far-infrared-reflectance[17] measurements gave different apparent gap values, which were interpreted[17] as possibly arising from c-axis versus ab-plane gap anisotropy. However, more recent tunneling experiments[18] are consistent with an isotropic gap and strong-coupling electron-phonon BCS behavior.

Whether the gaps in the above materials are indeed anisotropic in the above fashion can only be decided by repeated experiments in different laboratories on high-quality, untwinned single crystals. If, as the consistency of the experiments improves, some of the materials are found conclusively to have a c-axis versus ab-plane gap anisotropy, it would be helpful in interpreting the data to investigate the possible origin of such anisotropy.

In this work, we have investigated the competing roles of inter- and intralayer pairing with $N=1,2$ conducting layers per unit-cell edge s. We find that, for s-wave intralayer pairing only, the resulting gap is isotropic, even in the presence of single-particle interlayer hopping processes, which includes Josephson tunneling. Hence, for substantial gap anisotropy between wave vectors in the $\hat{c}$ and ab-plane directions to occur, the pairing must involve a spatial separation in the $\hat{c}$ direction of the paired fermions. Furthermore, such substantial gap anisotropy can only occur for $N \geq 2$, as the gap is always isotropic (or nearly so) for $N=1$, even when arising from interlayer pairing.

In Sec. II, we present and discuss the model, diagonalize the single-particle Hamiltonian for $N=1,2$, and solve the resulting mean-field equations. In Sec. III, we consider the $N=1$ case, solving for the gap functions and the OP's. We then generate the effective Ginzburg-Landau (GL) free energy, and minimize it to obtain the gap. In Sec. IV, we consider the $N=2$ case, obtaining the OP's, their T_c values, and their associated normalized gap functions. In Sec. V, we analyze the GL free energy for $N=2$, and the resulting gap as a function of the material parameters. In Sec. VI, we discuss our results. We also suggest experiments to help clarify our understanding of the high-T_c materials.

II. THE MODEL

We propose a model for the high-T_c superconductors that is sufficiently general so as to encompass all of the known materials that are superconducting, and which specifically addresses the issue of c-axis versus ab-plane gap anisotropy. We assume the quasiparticles (or quasiholes) are fermions, and that the normal state just above T_c for the superconducting materials is a Fermi liquid.[13,14,19] The sharpness and the magnitude of the observed Fermi edge in the Bi 2:2:1:2 photoemission experiments,[13,14] plus the remarkable agreement of its location with band-structure calculations,[20] convinces us that a true, rather conventional Fermi surface exists. A preliminary report[21] of de Haas-van Alphen measurements in Y 1:2:3 is also supportive of the sharp Fermi surface picture, as are positron-annihilation experiments.[19] Although, at present, a complete microscopic theory for the linear quasiparticle inelastic lifetime has not been presented, we believe that this effect is, at best, only marginally related to the magnitude of the discontinuity in the Fermi edge, which we assume to be conventional.

The layers between the conducting CuO_2 layers are assumed to be insulating. This assumption is supported in Y 1:2:3 by far-infrared-reflectance measurements[3] for $\mathbf{E}\|\hat{c}$ and by the T dependence of the normal-state resistivity tensor.[22] In Bi 2:2:1:2, the large normal-state-resistivity anisotropy[23] demands that the Sr-O and Ca-O layers be insulating. The Cu-O chain layer in Y 1:2:3 and the Bi-O layers in Bi 2:2:1:2 may count as additional conducting layers, as discussed below.

We assume there are $N \geq 1$ identical conducting layers per unit-cell edge s in the $\hat{c}$ direction, with $N-1$ interlayer spacings d, and one interlayer spacing $d'=s-(N-1)d$, respectively. The quasiparticles propagate freely with effective mass m_0 within each of the N conducting layers within the M unit cells, and tunnel (or hop) with effective matrix elements J_1 and J_2 between adjacent conducting planes within the same and neighboring unit cells (with separations d and d'), respectively. This assumption is strongly supported by band-structure calculations,[20] magnetic torque experiments,[24] and magnetization measurements[2] of the azimuthal dependence of the critical fields parallel to the layers, which are consistent with a corrugated cylindrical Fermi surface, with no significant anisotropy within the ab planes for $T \leq T_c$. In any event, $W_\perp/W_\| \ll 1$, where $W_\perp$ and $W_\|$ are the bandwidths for propagation perpendicular and parallel to the layers, respectively.

Within a given layer, the quasiparticles interact via the s-wave BCS pairing interaction λ_0. Quasiparticles on adjacent layers interact via BCS-like pairing interactions λ_1 and λ_2, for pairs on neighboring layers within the same and adjacent unit cells, respectively. This is pictured for $N=2$ in Fig. 1. For $N=1$, there is no intracell interlayer hopping or pairing, so we set $J_1=d=\lambda_1=0$.

Since a proper treatment of the role of the magnetic

field will be given in a subsequent publication, we neglect it entirely, except in the Appendix, where we have kept the Zeeman splitting of the quasiparticle energy for future reference. We use units in which $\hbar = k_B = c = 1$ in the following. This model and a compact summary of our results have been presented elsewhere.[25]

The quasiparticle Hamiltonian is thus taken to be $H = H_0 + V$, where

$$H_0 = s \int d^2r \Psi^\dagger(\mathbf{r}) \hat{\xi}_\sigma(\mathbf{r}) \Psi(\mathbf{r}) , \tag{1a}$$

$$V = \tfrac{1}{2} s \int d^2r \rho^\dagger(\mathbf{r}) \hat{V} \rho(\mathbf{r}) , \tag{1b}$$

where $\Psi(\mathbf{r})$ is a $2MN$-dimensional Nambu spinor with spinor component $\Psi_{jn}(\mathbf{r})$ which annihilates a quasiparticle at position $\mathbf{r}$ on the nth layer in the jth unit cell, $\rho(\mathbf{r})$ is an MN-dimensional density operator with component $\rho_{jn}(\mathbf{r}) = \Psi^\dagger_{jn}(\mathbf{r}) \Psi_{jn}(\mathbf{r})$,

$$\hat{\xi}_\sigma(\mathbf{r}) = [\xi_0(\mathbf{r}) \hat{1} + J_1 \hat{\delta}_1 + J_2 \hat{\delta}_2] \sigma_0 , \tag{1c}$$

$$\hat{V} = -\lambda_0 \hat{1} - \lambda_1 \hat{\delta}_1 - \lambda_2 \hat{\delta}_2 , \tag{1d}$$

and

$$\xi_0(\mathbf{r}) = -\nabla^2/(2m_0) - E_F , \tag{1e}$$

where E_F is the Fermi energy, σ_0 is the Pauli spin identity matrix, and $\hat{1}$, $\hat{\delta}_1$, and $\hat{\delta}_2$ are matrices of rank NM with elements given by

$$(\hat{1})^{jj'}_{nn'} = \delta_{jj'} \delta_{nn'} , \tag{2a}$$

$$(\hat{\delta}_1)^{jj'}_{nn'} = \delta_{jj'} (\delta_{n',n+1} + \delta_{n',n-1}) , \tag{2b}$$

and

$$(\hat{\delta}_2)^{jj'}_{nn'} = \delta_{j',j+1} \delta_{n'1} \delta_{nN} + \delta_{j',j-1} \delta_{n'N} \delta_{n1} . \tag{2c}$$

This model is similar to those considered previously by other authors.[26–37] With three exceptions,[26,31,33] none of those authors calculated the energy gap, however, as they were all concerned with the T_c behavior. The $N = 1$ version of this model was studied by Efetov and Larkin[26] and by Klemm and Scharnberg,[27] who calculated the upper critical field H_{c2}, including intralayer elastic scattering. Gulásci, Gulásci, and Pop[28] and Schneider and Baeriswyl[29] also studied the $N = 1$ version of this model in order to determine if the interlayer pairing would enhance the T_c value obtained from intralayer pairing. A generalization to $N > 1$ of their results was made by Ihm and Yu.[30] They[28–30] concluded that the intralayer and interlayer OP's would mix linearly, raising the T_c value above that of the maximum bare T_c value. This is questionable,[27] as pointed out recently by Suwa, Tanaka, and Tsukada[31] (STT), and in a treatment that neglected the important triplet OP by Schneider, De Raedt, and Frick.[32] STT correctly showed that such a T_c enhancement can only occur if the intralayer conduction band violates particle-hole symmetry (i.e., the linear coupling between the intra- and interlayer OP's is proportional to the derivative of the density of states at the Fermi energy). Such a scenario could arise for the tight-binding $N = 1$ intralayer band STT considered, for certain band fillings. However, their results led to an anomalous azimuthal dependence of H_{c2}, which is contrary to experiment.[2,24] In addition, STT included both intra- and interlayer pairing exchange terms in their Hamiltonian. While exchange is to be expected for on-site intralayer pairing, because it arises from the Pauli exclusion principle, it is not appropriate for interlayer pairing. Only in the unlikely situation that the interlayer pairing were of magnetic origin could it exhibit any significant spin dependence. Our model is easily generalized to arbitrary forms for the intralayer propagation energy $\xi_0(\mathbf{r})$, which, for $W_\perp / W_\parallel \ll 1$, leaves our results unaltered.

Tešanović[33] studied the $N = 1$ version of this model, adding a term due to interlayer pair hopping (or Josephson scattering). Since interlayer pair hopping is a selection of processes arising from intralayer pairing plus interlayer single quasiparticle hopping, the inclusion of such an additional interaction amounts to overcounting. More extensive overcounting in the Hamiltonian was made by Bulaevskii and Zyskin.[34] In addition, interlayer pair hopping implicitly violates time-reversal invariance, as the pairs must propagate in the same direction during the interlayer hopping. Similar models were studied by Appel and Fay[35] for $N = 1$ and by Jha[36] for $N > 1$. Since Appel and Fay did not discuss the T_c enchancement due to OP mixing, their results are essentially correct for their model. Jha's results and those of Birman and Lu[37] were questionable, as they did not properly diagonalize the free energy. Since the crystal is *periodic* in the unit-cell edge s, one must first Fourier transform in the layer index, and then diagonalize the resulting $N \times N$ matrix,[38] resulting in the T_c value corresponding to the average pairing interaction in the conducting layers in the unit cell. We note that experiments[39] on the Tl compounds reveal that T_c is not just a function of N, but depends upon many factors.

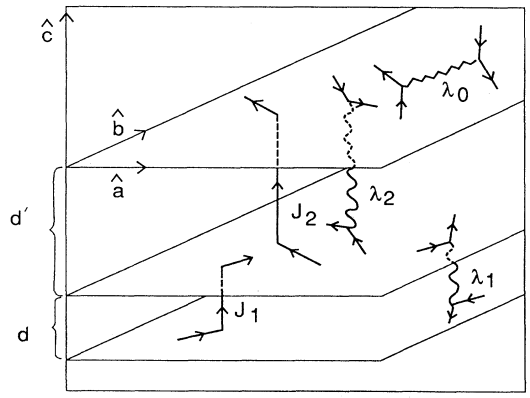

FIG. 1. Cross-sectional view of an $N = 2$ crystal section. The quasiparticles hop with matrix elements J_1 and J_2 between neighboring layers separated by d and $d' = s - d$, respectively. The intra- and interlayer pairing interactions λ_0, λ_1, and λ_2 are also pictured.

The model described by Eq. (1) could arise physically from a variety of possible mechanisms, prominent among which is the electron-phonon interaction. While numerous authors have proclaimed the impossibility of phonons playing a significant role in the mechanism for high-T_c superconductivity, recent experiments[40–45] lead us to suspect that this conventional wisdom may be misguided. The phonon dispersions have been determined for nonsuperconducting La_2CuO_4 (Ref. 40) and La_2NiO_4 (Ref. 40), and for superconducting $La_{2-x}Sr_xCuO_4$,[40,41] twinned Y 1:2:3,[41] and $Nd_{2-x}Ce_xCuO$ (Ref. 42) by neutron scattering. In Y 1:2:3 (Ref. 7) and $Nd_{2-x}Ce_xCuO_4$,[18] tunneling measurements of the electronic density of states yielded apparent strong-coupling anomalies, which appear to be consistent with the peaks in the phonon density of states obtained from neutron scattering.[42] In addition, the apparent lack of an appreciable isotope effect in Y 1:2:3 cannot be a valid reason for elimination of phonons as the mechanism, as demonstrated dramatically in the ^{18}O isotope experiments[43] on $La_{2-x}Sr_xCuO_4$. Similar ^{18}O isotope experiments[44] on Y 1:2:3 doped with Pr are also suggestive of a prominent role for the electron-phonon interaction in that system.

Velocity-of-sound measurements show strong anomalies[45] at T_c in $La_{2-x}Sr_xCuO_4$ and in Y 1:2:3. Ion-channeling measurements[46] on Y 1:2:3 have been interpreted as showing an anomalous change in the Debye-Waller factor at or near to T_c. This interpretation is supported by recent neutron-scattering measurements[47] of the Debye-Waller factor of the Cu ions in Bi 2:2:1:2, which show a kink in the T dependence of the Cu Debye-Waller factor at T_c, the sign of which is polarization dependent. More recent neutron-scattering experiments[47] showed a dramatic broadening of a phonon linewidth at T_c in Bi 2:2:1:2. Together these experiments suggest that phonons and/or charge fluctuations are strongly involved in the superconducting transition.

We note that the short coherence length $\xi_c(0)$ normal to the layers that has been inferred[2,24,48] does *not* limit the range of the pairing interaction to this value. Rather, it merely reflects the low value of the Fermi velocity along $\hat{\mathbf{c}}$, which depends upon J_1, J_2.

III. ABSENCE OF GAP ANISOTROPY FOR $N=1$

We now return to the Hamiltonian [Eq. (1)]. The single quasiparticle Hamiltonian H_0 may be diagonalized for arbitrary J_1, J_2, N by employing the periodicity of the lattice in the c- axis direction, as required by Bloch's theorem,

$$\Psi_{jn}(\mathbf{r})=(MsL_xL_y)^{-1/2}\times\sum_k \exp(i\mathbf{k}\cdot\mathbf{r})\times\exp\{ik_z[js+(n-1)d]\}\Psi_n(k)\ , \quad (3)$$

where $n\le N$, $k\equiv(\mathbf{k},k_z)$, L_xL_y is the area of the ab planes, and the Nambu spinor $\Psi_n(k)$ contains elements $\psi_{n\alpha}(k)$ for $\alpha=\pm$, which satisfy the usual fermion anticommutation relations,

$$\{\psi_{n\alpha}(k),\psi^\dagger_{n'\beta}(k')\}=\delta_{k_zk_z'}\delta_{nn'}\delta_{\alpha\beta}\delta^2(\mathbf{k}-\mathbf{k}')\ ,$$

etc.

For $N=1$, H_0 is diagonalized by the above procedure alone, leading to

$$H_0=(MsL_xL_y)^{-1}\sum_k \Psi^\dagger(k)\hat{\xi}_\sigma(k)\Psi(k)\ , \quad (4)$$

where $\Psi(k)\equiv\Psi_1(k)$, and

$$\hat{\xi}_\sigma(k)=[\xi_0(\mathbf{k})+2J_2\cos k_zs]\sigma_0\ ,$$

where $\xi_0(\mathbf{k})=\mathbf{k}^2/(2m_0)-E_F$. The Fermi surface is given by $\xi_0(\mathbf{k}_F)+2J_2\cos k_{zF}s=0$, which is a corrugated cylinder pictured in Fig. 2(a). The above Fourier transformation is then applied to the operators in the interaction V.

For $N=1$, the components of the temperature-ordered Green's function matrix in the Heisenberg representation are defined in the usual fashion,

$$G_{\alpha\beta}(k,\tau-\tau')\equiv-\langle T[\psi_\alpha(k,\tau)\psi^\dagger_\beta(k,\tau')]\rangle\ , \quad (5a)$$

$$F_{\alpha\beta}(k,\tau-\tau')\equiv\langle T[\psi_\alpha(k,\tau)\psi_\beta(-k,\tau')]\rangle\ , \quad (5b)$$

etc. Letting the Pauli matrices ρ_i and σ_i (and the identity matrices ρ_0 and σ_0) represent the usual[49] Green's function components (i.e., G, F, $F^\dagger$, and $-G^\dagger$) and the quasi-

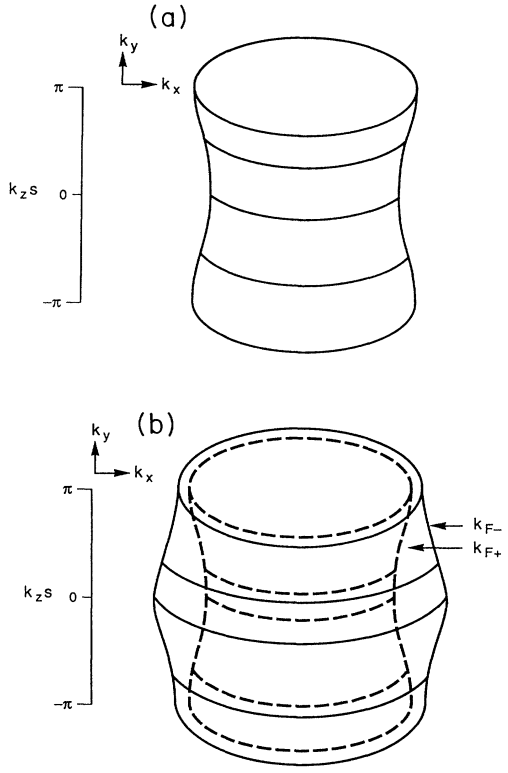

FIG. 2. The Fermi surface in the first zone $-\pi\le k_zs\le\pi$ is pictured. The corrugations in the c-axis direction are exaggerated for clarity. (a) $N=1$, (b) $N=2$.

particle spin, respectively, and using the standard mean-field decoupling procedure[50] for the interaction terms, the inverse temperature Green's function is a 4×4 matrix of the SU(2)×SU(2) form,

$$\hat{G}^{-1}(k,\omega)=i\omega\rho_0\sigma_0-[\xi_0(\mathbf{k})+2J_2\cos k_z s]\rho_3\sigma_0 -(\Delta_0'\rho_1-\Delta_0''\rho_2)\sigma_2 -\sum_{j=0}^{3}(\Delta_{3j}'\rho_1-\Delta_{3j}''\rho_2)\sigma_j \ , \tag{6}$$

where ω represents the Matsubara frequencies, Δ_0', Δ_0'', and Δ_{3j}', Δ_{3j}'' represent the real and imaginary parts of the intralayer pairing OP Δ_0 and the interlayer pairing gap functions Δ_{3j}. These are given for weak coupling by

$$\Delta_0=-\tfrac{1}{4}T\sum_{|\omega|\le\omega_\parallel}\int\frac{d^3k'}{(2\pi)^3}\lambda_0\mathrm{Tr}[(\rho_1-i\rho_2)\sigma_2\hat{G}(k',\omega)] \tag{7a}$$

and

$$\Delta_{3j}(k_z)=-\tfrac{1}{4}T\sum_{|\omega|\le\omega_\perp}\int\frac{d^3k'}{(2\pi)^3}V(k_z,k_z')\times\mathrm{Tr}[(\rho_1-i\rho_2)\sigma_j\hat{G}(k',\omega)] \ , \tag{7b}$$

where

$$V(k_z,k_z')=\lambda_2\cos[(k_z-k_z')s] \tag{7c}$$

is the Fourier transform of the mean-field interlayer pairing interaction, and $\int d^3k\equiv\int d^2k\int_{-\pi/s}^{\pi/s}dk_z$. In Eq. (7), we have separated the singlet functions Δ_0 and $\Delta_{32}(k_z)$. Although one could combine Δ_0 and Δ_{32} in one equation,[32] the orthogonality of Δ_0 with $\Delta_{32}(k_z)$ over the zone $-\pi/s\le k_z\le\pi/s$ allows us to write the gap-function equations as in Eq. (7). In addition, as the intralayer and interlayer pairing interactions arise in general from distinct microscopic processes[27] (including different phonon density-of-state weighting factors), they generally have distinct high-frequency cutoffs $\omega_\parallel$ and $\omega_\perp$, respectively. We note that $\Delta_{30}(k_z)$, $\Delta_{31}(k_z)$, and $\Delta_{33}(k_z)$ are triplet interlayer gap functions, as their spin configurations are represented by the symmetric matrices σ_0, σ_1, and σ_3.

We first consider the case of purely intralayer pairing ($\lambda=0\neq\lambda_0$). For this case, the only OP is Δ_0, which is independent of k_z. Even in the presence of interlayer quasiparticle tunneling (which includes Josephson tunneling), the gap $2|\Delta_0|$ for intralayer s-wave pairing is isotropic. For this OP, the Green's function matrix is readily inverted, as in textbooks.[49] After integration over $\xi_0(\mathbf{k}')$ and k_z', we obtain the standard BCS gap equation for Δ_0,

$$\Delta_0=\lambda_0N(0)\pi T\sum_{|\omega|\le\omega_\parallel}\frac{\Delta_0}{[\omega^2+|\Delta_0|^2]^{1/2}} \ , \tag{8a}$$

where $N(0)=m_0/(2\pi s)$ is the single quasiparticle density of states at the Fermi energy. The bare transition temperature T_{c0} (at which Δ_0 becomes nonvanishing in the absence of the interlayer gap functions) is given[51,52] by the weak-coupling BCS formula

$$1=\lambda_0N(0)\ln(2\gamma\omega_\parallel/\pi T_{c0}) \ , \tag{8b}$$

where $\gamma\approx1.78$ is the exponential of Euler's constant.

Next, we treat the case of purely interlayer pairing, setting $\lambda_0=0\neq\lambda_2$. The interlayer gap functions are best treated as components of a four-vector gap function $\tilde{\Delta}_3(k_z)$,

$$\tilde{\Delta}_3(k_z)\equiv(i\Delta_{30}(k_z),\Delta_{31}(k_z),\Delta_{32}(k_z),\Delta_{33}(k_z)) \ . \tag{9}$$

In this notation, $\Delta_{30}(k_z)$ is timelike, whereas the remaining gap functions are spacelike in the standard relativistic four-vector representation.

In the Appendix, we show that the four gap-function equations for the $\tilde{\Delta}_{3j}$ are best written as a single four-vector gap-function equation. To order $\tilde{\Delta}_3^3$, we find

$$\tilde{\Delta}_3(k_z)=\tfrac{1}{2}N(0)Ts\sum_{|\omega|\le\omega_\perp}\int_{-\pi/s}^{\pi/s}dk_z'V(k_z,k_z')\left[\frac{\tilde{\Delta}_3}{|\omega|}-(2\tilde{\Delta}_3|\tilde{\Delta}_3|^2-\tilde{\Delta}_3^*\tilde{\Delta}_3^2)/(2|\omega|^3)\right] \ . \tag{10}$$

where $V(k_z,k_z')$ is given by Eq. (7c), and $\tilde{\Delta}_3^*$ is the complex conjugate of $\tilde{\Delta}_3$. Inside the large parentheses on the right-hand side, $\tilde{\Delta}_3=\tilde{\Delta}_3(k_z')$. The standard four-vector scalar products are defined in the Appendix.

It is useful to write the interaction $V(k_z,k_z')$ as

$$V(k_z,k_z')=\lambda_2(\cos k_zs\cos k_z's+\sin k_zs\sin k_z's) \ . \tag{11}$$

For antisymmetric pair wave functions, $\tilde{\Delta}_{32}(k_z)$ is even in k_z and the remaining $\tilde{\Delta}_{3j}(k_z)$ are odd in k_z. Hence,

$$\tilde{\Delta}_{32}(k_z)=\sqrt{2}\Delta_s\cos k_zs \ , \tag{12a}$$

$$\tilde{\Delta}_{31}(k_z)=\sqrt{2}\Delta_{t0}\sin k_zs \ , \tag{12b}$$

$$\tilde{\Delta}_{\uparrow\uparrow}(k_z)=[\tilde{\Delta}_{30}(k_z)+i\tilde{\Delta}_{33}(k_z)]/\sqrt{2} =\sqrt{2}\Delta_{t+}\sin k_zs \ , \tag{12c}$$

and

$$\tilde{\Delta}_{\downarrow\downarrow}(k_z)=[\tilde{\Delta}_{30}(k_z)-i\tilde{\Delta}_{33}(k_z)]/\sqrt{2} =\sqrt{2}\Delta_{t-}\sin k_zs \ . \tag{12d}$$

In Eq. (12), Δ_s and the Δ_{tm} are complex quantities, independent of k_z. We define Δ_s to be the interlayer singlet OP. We then define the interlayer triplet vector OP to be

$$\Delta_t=\sum_{m=+,0,-}\hat{\mathbf{e}}_m\Delta_{tm} \ , \tag{13}$$

where $\{\hat{\mathbf{e}}_m\}$ forms an orthonormal vector set. The subscript m of Δ_{tm} is the magnetic quantum number of the

spin-1 OP.

The factors $\sqrt{2}$ on the right-hand side of Eq. (12) insure that the gap functions ($\sqrt{2}\cos k_z s$ and $\sqrt{2}\sin k_z s$) are properly normalized over the first zone $-\pi/s \le k_z \le \pi/s$. These normalized gap functions are orthogonal to each other and to unity (the gap function for intralayer pairing) within the first zone. We note that each of these two normalized gap functions vanishes for a particular value of k_z within the first zone, which might lead one naively to expect the resulting energy gap to exhibit a line node. However, such a scenario is forbidden on energetic grounds, as shown below.

The bare transition temperatures T_{cs} and T_{ct} for the singlet and triplet OP's are found from the part of Eq. (10) linear in the appropriate component of $\tilde{\Delta}_3$, leading to the result[26,27] $T_{cs}=T_{ct}=T_{c3}$, where

$$1=\tfrac{1}{2}\lambda_2 N(0)\ln(2\gamma\omega_\perp/\pi T_{c3}) \ . \tag{14}$$

One might think this result ($T_{cs}=T_{ct}$) is not so significant, as the nodal structure of the interlayer gap functions is incompatible with nonmagnetic intralayer impurity scattering. However, it has been shown previously[27] that T_{cs} and T_{ct} are *equally* suppressed by elastic intralayer nonmagnetic impurity scattering, at least in the self-consistent Born approximation. Hence, the relation $T_{cs}=T_{ct}$ holds, even in the presence of impurities, although the form of Eq. (14) is modified to the standard pair-breaking form.[27]

The free energy may be obtained as a power series in the various OP's from each of the components of Eq. (10), performing the integrals over k_z', and functionally integrating the resulting equation for Δ_s with respect to Δ_s^*, and that for Δ_{tm} with respect to Δ_{tm}^*. The free energy relative to the normal state is defined to be

$$F_S-F_N\equiv\tfrac{1}{2}N(0)(f_3+\delta f_{30}) \ , \tag{15a}$$

where f_3 is the part with $\Delta_0=0$, and δf_{30} includes all Δ_0 contributions. In the GL regime, we find, for weak coupling,

$$f_3=(|\Delta_s|^2+|\mathbf{\Delta}_t|^2)\ln(T/T_{c3}) + b_0\{\tfrac{3}{4}|\Delta_s|^4+\tfrac{3}{4}[2(|\mathbf{\Delta}_t|^2)^2-\mathrm{Re}(\mathbf{\Delta}_t^{*2}\mathbf{\Delta}_t^2)] + \tfrac{1}{2}[2|\Delta_s|^2|\mathbf{\Delta}_t|^2-\mathrm{Re}(\Delta_s^{*2}\mathbf{\Delta}_t^2)]\} \ , \tag{15b}$$

where $b_0=7\zeta(3)/[8(\pi T)^2]$. The coefficients $\frac{3}{4}$, $\frac{3}{4}$, and $\frac{1}{2}$ arise from the zone averages of $4\cos^4 x$, $4\sin^4 x$, and $8\cos^2 x\sin^2 x$, plus the functional integration of the gap-function equations. The quantity b_0 is the standard GL coefficient arising from $\pi T\sum_\omega|\omega|^{-3}/2$.

It is easy to minimize f_3 by considering its symmetry. First of all, f_3 is minimized when Δ_s and each of the components of $\mathbf{\Delta}_t$ are either in phase or π out of phase. The resulting phase minimized f_3 is then only a function of $|\Delta_s|$ and $|\mathbf{\Delta}_t|$. We assume $|\Delta_s|=|\mathbf{\Delta}_t|/\sqrt{x}=|\Delta|/\sqrt{2}\neq 0$. The minimum f_3 value $f_3^*=-\chi t^2/b_0$, where $t=\ln(T/T_{c3})$, and

$$\chi(x)=\frac{(x+1)^2}{3(1+x^2)+2x} \ . \tag{16}$$

The absolute maximum of $\chi(x)$ is $\frac{1}{2}$, which occurs at $x=1$. Hence, $|\Delta_s|=|\mathbf{\Delta}_t|$, and all three components of $\mathbf{\Delta}_t$ are equally probable.

It is important to note that, for this energetically favored configuration, the actual energy gap $2|\Delta|$ is *isotropic*,[26] as we have

$$|\tilde{\Delta}_3(k_z)|^2/2=|\Delta_s\cos(k_z s)|^2 + |\mathbf{\Delta}_t\sin(k_z s)|^2=|\Delta|^2/2 \ , \tag{17}$$

which is independent of k_z.

We now consider the possibility of $\tilde{\Delta}_3$ and Δ_0 simultaneously nonvanishing. From Eq. (6), it is clear that Δ_0 and $\tilde{\Delta}_3$ can be treated simultaneously by letting $\tilde{\Delta}_{32}\to\tilde{\Delta}_{32}+\Delta_0$ in the determinant of $\hat{G}^{-1}$. The full gap-function equations for this general case are given in Eq. (A11) of the Appendix. To cubic order in $\tilde{\Delta}_{3j}$ and Δ_0, we obtain

$$\Delta_0=\tfrac{1}{2}N(0)sT\lambda_0\sum_{|\omega|\le\omega_\parallel}\int_{-\pi/s}^{\pi/s}dk_z'\left[\frac{\Delta_0}{|\omega|}-[\Delta_0(|\Delta_0|^2+2|\tilde{\Delta}_3|^2)-\Delta_0^*(\tilde{\Delta}_3^2-2\tilde{\Delta}_{32}^2)]/(2|\omega|^3)\right] \tag{18a}$$

and

$$\tilde{\Delta}_{3j}(k_z)=\tfrac{1}{2}N(0)sT\sum_{|\omega|\le\omega_\perp}\int_{-\pi/s}^{\pi/s}dk_z'V(k_z,k_z')\left[\frac{\tilde{\Delta}_{3j}}{|\omega|}-\{2\tilde{\Delta}_{3j}(|\tilde{\Delta}_3|^2+|\Delta_0|^2)-\tilde{\Delta}_{3j}^*[\tilde{\Delta}_3^2+(1-2\delta_{j2})\Delta_0^2]\}/(2|\omega|^3)\right] \ , \tag{18b}$$

where the $\tilde{\Delta}_{3j}$ inside the square brackets are functions of k_z'.

Performing the integration over k_z' and the appropriate functional integrations, we find that the GL free energy is given by Eq. (15a), where f_3 is given by Eq. (15b) and

$$\delta f_{30}=|\Delta_0|^2\ln(T/T_{c0}) + b_0\{\tfrac{1}{2}|\Delta_0|^4+2|\Delta_0|^2(|\Delta_s|^2+|\mathbf{\Delta}_t|^2) + \mathrm{Re}[\Delta_0^{*2}(\Delta_s^2-\mathbf{\Delta}_t^2)]\} \ . \tag{19}$$

For $T_{c0} \neq T_{c3}$, the assumption of Δ_0 and Δ both nonvanishing leads to a contradiction. Hence, whichever gap has the higher-T_c value wins the battle, destroying the other gap completely. At the special point $T_{c0}=T_{c3}$, the choice of nonvanishing gap is arbitrary. In either case, the gap is isotropic, with a BCS-like T dependence.

This result is in contradiction to recent results[32,34] obtained by omitting Δ_t. Those workers[32,34] found an anisotropic gap for $T_{c3} > T_{c0}$, and concluded that the interlayer and intralayer OP's would coexist, causing a T-dependent anisotropy. As shown above, however, their solution does not minimize the free energy. First of all, Δ_0 and Δ_s are $\pi/2$ out of phase. More important, Δ_t conspires with Δ_s to give an isotropic gap $2|\Delta|$. Either $2|\Delta|$ or $2|\Delta_0|$ is energetically favored over the pure singlet anisotropic gap $(2|\Delta_0+\sqrt{2}\Delta_s \cos k_z s|)$ they considered.

IV. ORDER PARAMETERS AND T_c VALUES FOR $N=2$

For $N=2$, we again employ Eq. (3), setting $n=1,2$. We let

$$\Psi_n(k)=\exp[\mp i\phi(k_z)/2][\tilde{\Psi}_+(k)\pm\tilde{\Psi}_-(k)]/\sqrt{2} , \quad (20a)$$

where $n=1$ (2) corresponds to the upper (lower) sign,

$$\tan[\phi(k_z)]=\frac{J_2\sin(k_z d')-J_1\sin(k_z d)}{J_2\cos(k_z d')+J_1\cos(k_z d)} , \quad (20b)$$

and define

$$\tilde{\Psi}(k)\equiv\begin{bmatrix}\tilde{\psi}_{++}(k)\\ \tilde{\psi}_{+-}(k)\\ \tilde{\psi}_{-+}(k)\\ \tilde{\psi}_{--}(k)\end{bmatrix} \quad (20c)$$

to be a four-vector with element $\tilde{\psi}_{S\alpha}(k)$, where $S=\pm$ indexes the band and $\alpha=\pm$ indexes the spin. The $\tilde{\psi}_{S\alpha}(k)$ satisfy the fermion anticommutation relations

$$\{\tilde{\psi}_{S\alpha}(k),\tilde{\psi}^{\dagger}_{S'\beta}(k')\}=\delta_{kk'}\delta_{SS'}\delta_{\alpha\beta} ,$$

etc.

The transformed single-quasiparticle Hamiltonian $\tilde{H}_0$ is then diagonal,

$$\tilde{H}_0=(MsL_xL_y)^{-1}\sum_k \tilde{\Psi}^{\dagger}(k)\hat{\tilde{\xi}}_{\mu\sigma}(k)\tilde{\Psi}(k) , \quad (21a)$$

where

$$\hat{\tilde{\xi}}_{\mu\sigma}(k)=\xi_0(\mathbf{k})\mu_0\sigma_0+\varepsilon_{\perp}(k_z)\mu_3\sigma_0 , \quad (21b)$$

μ_i and the identity matrix μ_0 are Pauli matrices representing the band degrees of freedom, and

$$\varepsilon_{\perp}(k_z)=(J_1^2+J_2^2+2J_1J_2\cos k_z s)^{1/2} . \quad (21c)$$

The two band dispersions are thus $\xi_0(\mathbf{k})\pm\varepsilon_{\perp}(k_z)$. This leads to two Fermi surfaces defined by $\xi_0(\mathbf{k}_{F\pm})\pm\varepsilon_{\perp}(k_{zF\pm})=0$, which are pictured in Fig. 2(b). As for $N=1$, the operators in V [Eq. (1b)] are Fourier transformed, but for $N=2$ we must also rotate them [Eq. (20a)] in order to diagonalize H_0.

For $N=2$, it is necessary to define the temperature-ordered Green's-function components in the Heisenberg *band* representation,

$$\tilde{G}^{\alpha\beta}_{SS'}(k,\tau-\tau')\equiv\langle T[\tilde{\psi}_{S\alpha}(k,\tau)\tilde{\psi}^{\dagger}_{S'\beta}(k,\tau')]\rangle , \quad (22a)$$

$$\tilde{F}^{\alpha\beta}_{SS'}(k,\tau-\tau')\equiv\langle T[\tilde{\psi}_{S\alpha}(k,\tau)\tilde{\psi}_{S'\beta}(-k,\tau')]\rangle , \quad (22b)$$

etc. In the mean-field approximation, the inverse temperature Green's function is an 8×8 matrix of $SU(2)\times SU(2)\times SU(2)$ form,

$$\hat{\tilde{G}}^{-1}(k,\omega)=i\omega\rho_0\mu_0\sigma_0-\xi_0(\mathbf{k})\rho_3\mu_0\sigma_0-\varepsilon_{\perp}(k_z)\rho_3\mu_3\sigma_0-\sum_{i=0}^{1}(\Delta_i'\rho_1-\Delta_i''\rho_2)\mu_i\sigma_2$$
$$-\sum_{i=2}^{3}\sum_{j=0}^{3}(\Delta_{ij}'\rho_1-\Delta_{ij}''\rho_2)\mu_i\sigma_j-\sum_{\substack{i,k=2\\ i\neq k}}^{3}\sum_{j=0}^{3}(\bar{\Delta}_{ij}'\rho_1-\bar{\Delta}_{ij}''\rho_2)\mu_k\sigma_j , \quad (23)$$

where

$$\Delta_i=-\tfrac{1}{8}T\sum_{|\omega|\le\omega_{\parallel}}\int\frac{d^3k'}{(2\pi)^3}\lambda_0\mathrm{Tr}[(\rho_1-i\rho_2)\mu_i\sigma_2\hat{\tilde{G}}(k',\omega)] \quad (24a)$$

for $i=0$, 1, and

$$\Delta_{ij}(k_z)=-\tfrac{1}{8}T\sum_{|\omega|\le\omega_{\perp}}\int\frac{d^3k'}{(2\pi)^3}\tilde{V}'(k_z,k_z')\mathrm{Tr}[(\rho_1-i\rho_2)\mu_i\sigma_j\hat{\tilde{G}}(k',\omega)] , \quad (24b)$$

$$\bar{\Delta}_{ij}(k_z)=-\tfrac{1}{8}T\sum_{|\omega|\le\omega_{\perp}}\int\frac{d^3k'}{(2\pi)^3}\tilde{V}''(k_z,k_z')\mathrm{Tr}[(\rho_1-i\rho_2)\mu_i\sigma_j\hat{\tilde{G}}(k',\omega)] , \quad (24c)$$

for $i=2, 3$, where

$$\tilde{V}(k_z,k_z')=\lambda_1\exp\{i[(k_z-k_z')d+\phi(k_z)-\phi(k_z')]\}+\lambda_2\exp\{i[(k_z-k_z')d'-\phi(k_z)+\phi(k_z')]\} \tag{24d}$$

is the effective mean-field interlayer pairing interaction obtained by the Fourier transformation plus the rotation, and $\tilde{V}'$ and $\tilde{V}''$ are the real and imaginary parts of $\tilde{V}$, respectively. The intralayer singlet OP's Δ_0 and Δ_1 are independent of k_z. Δ_0 and the interlayer gap functions $\Delta_{3j}(k_z)$ are analogous to those for $N=1$, but Δ_1 and the interlayer gap functions $\Delta_{2j}(k_z)$ arise from the pairing of quasiparticles in *different* bands, as their band matrix structures are represented by μ_1 and μ_2, respectively. The additional anomalous gap functions $\bar{\Delta}_{2j}(k_z)$ and $\bar{\Delta}_{3j}(k_z)$ arise from mixed intra- and interband pairing processes. Since $\tilde{V}''(k_z',k_z)=-\tilde{V}''(k_z,k_z')$, these gap functions can only become nonvanishing from their coupling to *other* nonvanishing gap functions. In this paper, we neglect the $\bar{\Delta}_{ij}$ completely.

The classification of these $N=2$ interlayer gap functions is evident from the Pauli matrix structure of the Green's function matrix: singlet states (represented by σ_2) are odd in the spin configuration, whereas the triplet spin states (represented by σ_0, σ_1 and σ_3) are even in the spin configuration. Those states odd in the band index are represented by μ_2 and are not time-reversal invariant, whereas those states represented by μ_0, μ_1, and μ_3 are even in the band index and are invariant under time reversal. The remaining degrees of freedom are implicit in the k_z dependences of the pair wave functions. As the overall pair wave function must be odd under quasiparticle exchange, the symmetry of the k_z dependence of the gap functions is as follows: Δ_{20}, Δ_{21}, Δ_{23}, and Δ_{32} are *even* functions of k_z, whereas Δ_{22}, Δ_{30}, Δ_{31}, and Δ_{33} are *odd* functions of k_z.

We first consider the $N=2$ case of purely intralayer pairing ($\lambda_1=\lambda_2=0\neq\lambda_0$). For this case, the Green's function matrix given by Eq. (23) is readily inverted, as shown in the Appendix. Expanding Eq. (A10) to order Δ_i^3, we have

$$\Delta_0=\tfrac{1}{2}\lambda_0 N(0)sT\sum_{|\omega|\le\omega_\parallel}\int_{-\pi/s}^{\pi/s}dk_z'\left[\frac{\Delta_0}{|\omega|}-(\Delta_0|\Delta_0|^2+z_1\Delta_0^*\Delta_1^2+2z_2\Delta_0|\Delta_1|^2)/(2|\omega|^3)\right] \tag{25a}$$

and

$$\Delta_1=\tfrac{1}{2}\lambda_0 N(0)sT\sum_{|\omega|\le\omega_\parallel}\int_{-\pi/s}^{\pi/s}dk_z'\left[\frac{\Delta_1 z_1}{|\omega|}-(z_3\Delta_1|\Delta_1|^2+z_1\Delta_1^*\Delta_0^2+2z_2\Delta_1|\Delta_0|^2)/(2|\omega|^3)\right], \tag{25b}$$

where

$$z_1=1-\delta, \tag{25c}$$

$$z_2=(1-\delta)^2, \tag{25d}$$

$$z_3=(1-\delta)^2(1-4\delta), \tag{25e}$$

and

$$\delta=\frac{\varepsilon_\perp^2(k_z')}{\omega^2+\varepsilon_\perp^2(k_z')} \tag{25f}$$

describes a different type of pair breaking.

The bare transition temperature T_{c0} for the Δ_0 OP is obtained by linearizing Eq. (25a), which results in Eq. (8c). Similarly, the gap equation with only Δ_0 nonvanishing is obtained from Eq. (A10a) by setting $\Delta_1=0$, resulting in Eq (8a).

The bare transition temperature T_{c1}^0 for the Δ_1 OP is similarly obtained from the linear term in Eq. (25b),

$$\ln(T_{c1}^0/T_{c0})=\int_{-\pi}^{\pi}\frac{dx}{2\pi}\mathrm{Re}\{\psi(\tfrac{1}{2})-\psi[1/2+ig(x,T_{c1}^0)]\}, \tag{26a}$$

where

$$g(x,T)\equiv\varepsilon_\perp(x/s)/(2\pi T) \tag{26b}$$

and $\psi(z)$ is the digamma function. Equation (26a) has the standard pair-breaking form,[49] with the function $i\varepsilon_\perp(k_z)$ acting as the pair-breaking parameter. We shall refer to this type of pair breaking as *interband pair breaking*. We recall from Eq. (23) that Δ_0 arises from intralayer s-wave pairing between quasiparticles in the same band, but Δ_1 arises from intralayer s-wave pairing between quasiparticles in *different* bands. This difference is evident in the band Pauli matrix structure, represented by μ_0 and μ_1, respectively.

To leading order in J_i/T_{c0},

$$T_{c1}^0/T_{c0}\approx 1-7\zeta(3)(J_1^2+J_2^2)/(2\pi T_{c0})^2,$$

where $\zeta(z)$ is the Riemann ζ function. Hence, $T_{c1}^0<T_{c0}$, unless $J_1=J_2=0$. In materials with two nearby CuO_2 planes (e.g., Y 1:2:3) it is likely that $J_1/T_{c0}\gg 1$, implying $T_{c1}^0=0$. As shown in the Appendix, even when $T_{c1}^0\neq 0$, the nonvanishing Δ_0 acts as a very strong pair breaker upon Δ_1, driving its actual transition temperature T_{c1} essentially to 0.

We now consider the case of purely interlayer pairing, setting $\lambda_0=0$. For this case the nonvanishing quantities are Δ_{2j} and Δ_{3j}, as discussed above. As for the $N=1$ case, each of the two interlayer gap functions is a four-vector,

$$\tilde{\Delta}_2(k_z)\equiv i(i\Delta_{20}(k_z),\Delta_{21}(k_z),\Delta_{22}(k_z),\Delta_{23}(k_z)) , \quad (27)$$

and $\tilde{\Delta}_3(k_z)$ is defined by Eq. (9). The extra overall factor of i in Eq. (27) implies that there is one spacelike gap function $\tilde{\Delta}_{20}$; the other three gap functions are timelike.

We first consider the cases of $\tilde{\Delta}_2$ and $\tilde{\Delta}_3$ separately nonvanishing. From Eq. (A13) of the Appendix, the linearized gap-function equations are

$$\tilde{\Delta}_3(k_z)=\tfrac{1}{2}N(0)Ts\sum_{|\omega|\le\omega_\perp}\int_{-\pi/s}^{\pi/s}dk_z'\tilde{V}'(k_z,k_z')\frac{\tilde{\Delta}_3(k_z')}{|\omega|} \quad (28a)$$

and

$$\tilde{\Delta}_2(k_z)=\tfrac{1}{2}N(0)Ts\sum_{|\omega|\le\omega_\perp}\int_{-\pi/s}^{\pi/s}dk_z'\tilde{V}'(k_z,k_z')\times\frac{\tilde{\Delta}_2(k_z')z_1(k_z')}{|\omega|} , \quad (28b)$$

where z_1 and $\tilde{V}'(k_z,k_z')$ are given by Eqs. (25c) and (24d). Equation (28a) differs from the linearized Eq. (10) (for $N=1$) only in the form of the interaction. Equation (28b) also differs from Eq. (10) due to interband pair breaking. In addition, we note the similarity of Eq. (28) with the linearized Eqs. (25a) and (25b) for Δ_0 and Δ_1.

The transition temperatures T_{c3} and T_{c2} for the $\tilde{\Delta}_3$ and $\tilde{\Delta}_3$ gap functions may be found from Eq. (28). Since most of the interesting physics arises from the differences in the T_c's for the various gap functions, we present our results in detail.

We note that $\tilde{V}'(k_z,k_z')$ can be written as

$$\tilde{V}'(k_z,k_z')=\sum_{l=1,2}\sum_{S=\pm}\lambda_l|\psi_l^S(k_z)\rangle\langle\psi_l^S(k_z')| , \quad (29a)$$

where

$$|\psi_1^+(k_z)\rangle=\cos[k_zd+\phi(k_z)] , \quad (29b)$$

and

$$|\psi_2^+(k_z)\rangle=\cos[k_zd'-\phi(k_z)] , \quad (29c)$$

and where the $|\psi_l^-(k_z)\rangle$ functions are obtained from the above with the cosine functions being replaced by sine functions. Using Eq. (21b), it is easy to show that

$$|\psi_1^+(k_z)\rangle=[J_1+J_2\cos(k_zs)]/\varepsilon_\perp(k_z) , \quad (30a)$$

$$|\psi_2^+(k_z)\rangle=[J_1\cos(k_zs)+J_2]/\varepsilon_\perp(k_z) , \quad (30b)$$

$$|\psi_1^-(k_z)\rangle=J_2\sin(k_zs)/\varepsilon_\perp(k_z) , \quad (30c)$$

and

$$|\psi_2^-(k_z)\rangle=J_1\sin(k_zs)/\varepsilon_\perp(k_z)=(J_1/J_2)|\psi_1^-(k_z)\rangle . \quad (30d)$$

The $|\psi_l^\pm(k_z)\rangle$ are commensurate with the lattice. In addition, $|\psi_1^+(k_z)\rangle$ and $|\psi_2^+(k_z)\rangle$ are linearly independent, but not orthogonal over the first zone $(-\pi/s,\pi/s)$. Since $|\psi_2^-\rangle=(J_1/J_2)|\psi_1^-\rangle$, these two functions are equivalent. We define n_S to be the number of linearly independent even ($S=+$) or odd ($S=-$) eigenfunctions in $\tilde{V}'(k_z,k_z')$. Generally, we have $n_+=2$, $n_-=1$. For the special case $J_1=J_2$, however, $|\psi_1^+\rangle=|\psi_2^+\rangle$, so $n_+=1$.

We shall write the eigenfunctions for $J_2\ge J_1\ge 0$. Forms for $J_1\ge J_2\ge 0$ can be obtained by interchanging J_1 with J_2 and λ_1 and λ_2. We first define

$$\eta=(J_1/J_2)^2 \quad (31a)$$

and

$$\bar{\lambda}=(\lambda_1+\lambda_2\eta)/2 . \quad (31b)$$

Normalizing the odd eigenfunction, we obtain

$$|u_{31}^-(k_z)\rangle=\sqrt{2}J_2\sin(k_zs)/\varepsilon_\perp(k_z) \quad (31c)$$

and

$$\lambda_{31}^-=\bar{\lambda} . \quad (31d)$$

To obtain the even eigenfunctions, we first employ the standard Gram-Schmidt orthonormalization procedure to obtain an orthonormal basis

$$\{|\phi_l^+(k_z)\rangle\} \text{ from } \{|\psi_l^+(k_z)\rangle\} . \quad (32)$$

We then write the part of $\tilde{V}'(k_z,k_z')$ even in k_z,k_z' in terms of this basis. The resulting form can be diagonalized by a unitary transformation, equivalent to a rotation. The even eigenfunctions and eigenvalues are found to be

$$|u_{3n}^+(k_z)\rangle=(a_\pm+b_\pm\cos k_zs)/\varepsilon_\perp(k_z) , \quad (33a)$$

and

$$\lambda_{3n}^+=(\lambda_+\pm Z)/2 , \quad (33b)$$

where the upper (lower) signs correspond to $n=1$ (2),

$$\lambda_\pm=\bar{\lambda}\pm\zeta\lambda_2 , \quad (33c)$$

$$\zeta=1-\eta , \quad (33d)$$

$$Z=(\lambda_-^2+2\lambda_2^2\eta\zeta)^{1/2} , \quad (33e)$$

$$b_\pm=(1\pm\lambda_-/Z)^{1/2} , \quad (33f)$$

and

$$a_\pm=b_\pm\sqrt{\eta}\pm b_\mp\sqrt{\zeta/2} . \quad (33g)$$

We note that $\lambda_{31}^+>\lambda_{32}^+$ and that $\lambda_{31}^+\ge\lambda_{31}^-$. All of the eigenvalues are real.

In this representation, $\tilde{V}'(k_z,k_z')$ is diagonal, as well as separable in k_z and k_z',

$$\tilde{V}'(k_z,k_z')=\sum_{S=\pm}\sum_{n=1}^{n_S}\lambda_{3n}^S|u_{3n}^S(k_z)\rangle\langle u_{3n}^S(k_z')| . \quad (34)$$

Equation (34) is particularly useful for treating the states invariant under time reversal for *arbitrary* N. For $N=1$, Eq. (11) may also be written in this form, with $n_\pm=n_-=1$, $\lambda_{31}^+=\lambda_{31}^-=\lambda_2/2$, and $|u_{31}^S(k_z)\rangle$ given by $\sqrt{2}\cos k_zs$ and $\sqrt{2}\sin k_zs$, respectively.

We then write the $\tilde{\Delta}_{3j}(k_z)$ in terms of this orthonormal basis,

$$\tilde{\Delta}_{32}(k_z)=\sum_{n=1}^{2}\Delta_{32n}|u_{3n}^{+}(k_z)\rangle \tag{35a}$$

and

$$\tilde{\Delta}_{3j}(k_z)=\Delta_{3j1}|u_{31}^{-}(k_z)\rangle \tag{35b}$$

for $j\neq 2$. Using these forms in Eq. (28a), we obtain n_S T_{c3} values T_{c3n}^{S} given by

$$1=\lambda_{3n}^{S}N(0)\bar{a}(T_{c3n}^{S}) , \tag{36a}$$

where

$$\bar{a}(T)=\ln(2\gamma\omega_{\perp}/\pi T) . \tag{36b}$$

Since $\lambda_{31}^{+}>\lambda_{32}^{+}$ and $\lambda_{31}^{+}\geq\lambda_{31}^{-}$, we have $T_{c31}^{+}>T_{c32}^{+}$ and $T_{c31}^{+}\geq T_{c31}^{-}$. We let $T_{cs}=T_{c31}^{+}$ and $T_{ct}=T_{c31}^{-}$ be the higher singlet and the triplet T_c values, respectively. Hence, $T_{cs}\geq T_{ct}$, the equality holding only for special cases in the parameter space. For $J_1/J_2\leq 1$, these special cases are (a) $J_1/J_2=1$, (b) $\lambda_2=0$, and (c) $J_1=0$, and $\lambda_2/\lambda_1<\frac{1}{2}$. The fact that T_{cs} is otherwise greater than T_{ct} is the most important difference between the $N=1$ and 2 cases. The OP's corresponding to these T_c values are defined to be $\Delta_s=\Delta_{321}$ and Δ_t, which is a vector OP with components $\Delta_{t\pm}=(\Delta_{301}\pm i\Delta_{331})/\sqrt{2}$ and $\Delta_{t0}=\Delta_{311}$ as in Eq. (12) (see the Appendix).

In Fig. 3, we have plotted the orthonormal gap functions $|u_{3n}^{\pm}(k_z)\rangle$ as functions of $k_z s/\pi$. In each figure, the lettering (a)–(c) correspond to $|u_{31}^{+}\rangle$, $|u_{32}^{+}\rangle$, and $|u_{31}^{-}\rangle$, respectively. In the left figure, the parameters are $\lambda_1/\lambda_2=0.9$ and $J_1/J_2=0.7$. The relative eigenvalues $\lambda_{3n}^{\pm}/\lambda_2$ for these curves are (a) 0.9679, (b) 0.2371, and (c) 0.6950, respectively. We note that $|u_{31}^{+}(k_z)\rangle$ is nodeless, whereas the other gap functions each have a pair of nodes, and lower T_c values. In the right figure, the parameter values are $\lambda_2/\lambda_1=0.4$ and $J_1/J_2=0.8$. The relative eigenvalues $\lambda_{3n}^{\pm}/\lambda_1$ for these curves are (a) 0.6635, (b) 0.1085, and (c) 0.6280, respectively. In this figure, all curves have a pair of nodes. In each figure, we note that the odd eigenfunction has a node at $k_z=0$, and one-half of a node at $k_z=\pm\pi/s$. The second node disappears for $J_1/J_2=1$.

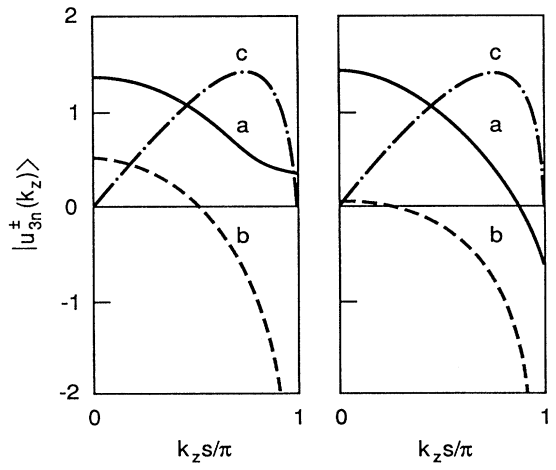

FIG. 3. Plotted are the orthonormal wave functions $|u_{3n}^{\pm}(k_z)\rangle$ as functions of $k_z s/\pi$ for the parameters $\lambda_1/\lambda_2=0.9$, $J_1/J_2=0.7$ and $\lambda_2/\lambda_1=0.4$, $J_1/J_2=0.8$ in the left-hand and right-hand figures, respectively. The curves (a), (b), and (c) refer, respectively, to $|u_{31}^{+}(k_z)\rangle$, $|u_{32}^{+}(k_z)\rangle$, and $|u_{31}^{-}(k_z)\rangle$. The relative eigenvalues $\lambda_{3n}^{\pm}/\lambda_2$ for the left-hand figure are (a) 0.9679, (b) 0.2371, and (c) 0.6950. In the right-hand figure, the relative eigenvalues $\lambda_{3n}^{\pm}/\lambda_1$ are (a) 0.6635, (b) 0.1085, and (c) 0.6280.

To calculate the bare T_{c2} values, we first expand $\tilde{\Delta}_{2j}(k_z)$ in its own orthonormal basis $\{|u_{2n}^{S}(k_z)\rangle\}$,

$$\tilde{\Delta}_{22}(k_z)=\Delta_{221}|u_{21}^{-}(k_z)\rangle \tag{37a}$$

and

$$\tilde{\Delta}_{2j}(k_z)=\sum_{n=1}^{2}\Delta_{2jn}|u_{2n}^{+}(k_z)\rangle , \tag{37b}$$

for $j\neq 2$. The linearized equation for Δ_{221} is then diagonal, with eigenvalue $\alpha_{21}^{-}(T)=a_{21}^{-}(T)$, where

$$a_{2n}^{S}(T)=[\lambda_{3n}^{S}N(0)]^{-1}-\bar{a}(T)-K_{nn}^{S}(T) , \tag{38a}$$

for $S=\pm$, where

$$K_{nn'}^{S}(T)=\int\frac{dx}{2\pi}\langle u_{3n}^{S}(x/s)|u_{3n'}^{S}(x/s)\rangle \times\mathrm{Re}\{\psi(\tfrac{1}{2})-\psi[1/2+ig(x,T)]\} , \tag{38b}$$

$g(x,T)$ is given by Eq. (26b) and $\psi(x)$ is the digamma function. The singlet eigenfunction $|u_{21}^{-}(k_z)\rangle=|u_{31}^{-}(k_z)\rangle$, which is *odd* in k_z. The triplet eigenfunctions $|u_{2n}^{+}(k_z)\rangle$ and eigenvalues $\alpha_{2n}^{+}(T)$ are listed in the Appendix.

For each eigenvalue $\alpha_{2n}^{S}(T)$, there is a corresponding bare T_{c2} value T_{c2n}^{S0} given by

$$\alpha_{2n}^{S}(T_{c2n}^{S0})=0 . \tag{39}$$

We rank order the T_{c2} values T_{c2n}^{S0} in decreasing order, with T_{c21}^{S0} corresponding to the highest-T_c value for a particular $S=\pm$ value, as for the λ_{3n}^{S} and the T_{c3n}^{S}. At fixed T, the $\alpha_{2n}^{S}(T)$ are then ranked in increasing order, as we have divided by $\lambda_{3n}^{S}N(0)$ in Eq. (38a). As for the intralayer pairing case, we find that the T_{c2n}^{S0} are suppressed from T_{c3n}^{S} by interband pair breaking. The suppression is given by

$$T_{c2n}^{S0}/T_{c3n}^{S}\approx 1-C_n^{S}(J/T_{c3n}^{S})^2 ,$$

where $J^2=J_1^2+J_2^2$, and $C_n^{S}>0$ is of order unity. Unless $J/T_{c3n}^{S}\ll 1$, we can neglect $\tilde{\Delta}_2$ altogether. Usually, the interband pair breaking is sufficiently strong ($J/T_{c3n}^{S}>1$) that all of the $T_{c2n}^{S0}=0$. Even for $T_{c2n}^{S0}\neq 0$, the nonvanishing Δ_s below T_{cs} acts as a sufficiently strong pair breaker upon the OP's in $\tilde{\Delta}_2$ as to force their amplitudes to vanish below T_{cs}, as shown in the Appendix.

To construct the GL free energy $\frac{1}{2}N(0)f$ in terms of the Δ_{ijn}, we need to find the eigenvalues at arbitrary T. The above procedure insures that the basis gap functions

are properly normalized. For terms in f, obtained from the $\tilde{\Delta}_3$ equation, we must also divide the coefficients of $|u^S_{3n}(k_z)\rangle$ by $\lambda^S_{3n}N(0)$. The resulting coefficients of the quadratic terms in f are

$$\alpha^S_{3n}(T)=\bar{a}(T^S_{c3n})-\bar{a}(T)=\ln(T/T^S_{c3n}) \tag{40a}$$

and

$$\alpha^S_{2n}(T)\equiv\ln(T/T^{S0}_{c2n})+\delta\alpha^S_{2n}(T)\ . \tag{40b}$$

From Eq. (40a), we have $\delta\alpha^S_{2n}(T^{S0}_{c2n})=0$.

We now consider simultaneous intra- and interlayer pairing. Since our separate analysis of the intra- and interlayer pairing cases resulted in pair breaking for the Δ_1 OP and for the $\tilde{\Delta}_{2j}$ gap functions, we neglect Δ_1 and $\tilde{\Delta}_{2j}$, which is certainly valid near the highest transition temperature. In the Appendix, we have treated Δ_0 and $\tilde{\Delta}_3$ to all orders simultaneously. Expanding Eqs. (A11a) and (A11b) to cubic order in Δ_0 and $\tilde{\Delta}_{3j}$, we find that the resulting gap-function equations are identical to Eqs. (18a) and (18b), with the modification that $V(k_z,k_z')$ is replaced by $\tilde{V}'(k_z,k_z')$ in Eq. (18b). This modification is responsible for T_{cs} and T_{ct} being generally distinct for $N=2$. Hence, there are three important T_c values: T_{c0}, T_{cs}, and T_{ct}, as discussed in Sec. V.

V. GINZBURG-LANDAU FREE ENERGY FOR $N=2$

From the analysis in the Appendix, the dominant part of the free energy $\frac{1}{2}N(0)f_{30}$ arises from Δ_0 and the Δ_s and $\boldsymbol{\Delta}_t$ OP's, defined for $N=2$ in the Appendix and below Eq. (36). We have

$$\begin{aligned}f_{30}=&|\Delta_s|^2\ln(T/T_{cs})+|\boldsymbol{\Delta}_t|^2\ln(T/T_{ct})+|\Delta_0|^2\ln(T/T_{c0})+\beta_s|\Delta_s|^4\\&+\beta_t[2(|\boldsymbol{\Delta}_t|^2)^2-\mathrm{Re}(\boldsymbol{\Delta}_t^{*2}\boldsymbol{\Delta}_t^2)]+2\beta_{st}[2|\Delta_s|^2|\boldsymbol{\Delta}_t|^2-\mathrm{Re}(\Delta_s^{*2}\boldsymbol{\Delta}_t^2)]\\&+b_0\{\tfrac{1}{2}|\Delta_0|^4+2|\Delta_0|^2(|\Delta_s|^2+|\boldsymbol{\Delta}_t|^2)+\mathrm{Re}[\Delta_0^{*2}(\Delta_s^2-\boldsymbol{\Delta}_t^2)]\}\ ,\end{aligned} \tag{41}$$

where $\beta_t=3b_0/4$, as for $N=1$, and β_s, β_{st} are given in the Appendix. The quantities T_{cs}/T_{ct}, β_s and β_{st} reduce to the $N=1$ values at $J_1/J_2=1$, but generally are functions of J_1/J_2 and λ_1/λ_2. The terms containing Δ_0 are identical to Eq. (19) for $N=1$.

As for $N=1$, the signs of the Δ_0, Δ_s and the Δ_0, $\boldsymbol{\Delta}_t$ coupling terms are different. For $N=1$ and 2 with $T_{cs}=T_{ct}$, this causes Δ_0 to be completely incompatible with the isotropic interlayer gap $2|\Delta|$. For $N=2$ and $T_{cs}>T_{ct}$, the situation is more complicated. To investigate the competition between Δ_0, Δ_s and $\boldsymbol{\Delta}_t$, we must consider all allowed orderings of T_{c0}, T_{cs}, and T_{ct}. As discussed below, it does not appear to be possible to have Δ_0, Δ_s, and $\boldsymbol{\Delta}_t$ simultaneously nonvanishing.

We first consider the case $T_{c0}>T_{cs}\geq T_{ct}$. Below T_{c0}, $|\Delta_0|\neq 0$. It is easily shown that the assumption of either $|\Delta_s|\neq 0$ or $|\boldsymbol{\Delta}_t|\neq 0$ below the temperatures $\tilde{T}_{cs}$ or $\tilde{T}_{ct}$ leads to a contradiction. We therefore conclude that, for $T_{c0}>T_{cs}\geq T_{ct}$, Δ_0 is the *only* nonvanishing OP, and the gap $2|\Delta_0|$ is isotropic.

We next consider the case $T_{cs}\geq\max(T_{ct},T_{c0})$. There are two cases of interest: $T_{cs}>T_{ct}$ and $T_{cs}=T_{ct}$. The $T_{cs}=T_{ct}$ case reduces to the case considered for $N=1$: $|\Delta_0|=0$, and the gap $2|\Delta|$ is isotropic, where $|\Delta_s|=|\boldsymbol{\Delta}_t|=|\Delta|/\sqrt{2}$. Hence, we assume $T_{cs}>\max(T_{ct},T_{c0})$.

Just below T_{cs}, the system is in the S phase,

$$|\Delta_s|^2=-t/(2\beta_s) \tag{42a}$$

and

$$|\boldsymbol{\Delta}_t|=|\Delta_0|=0\ . \tag{42b}$$

At lower T, we could have $\Delta_s\neq 0$ and either $\boldsymbol{\Delta}_t\neq 0=\Delta_0$ or $\Delta_0\neq 0=\boldsymbol{\Delta}_t$. We denote these phases the ST and SS phases, respectively. For T_{ct} and T_{c0} both finite, we must first determine which, if either, of these phases would be favored. Below T_{cs}, $|\Delta_s|\neq 0$ acts as a pair breaker upon both Δ_0 and $\boldsymbol{\Delta}_t$, suppressing T_{ct} and T_{c0} to $\tilde{T}_{ct}$ and $\tilde{T}_{c0}$, respectively.

We let $t=\ln(T/T_{cs})$, $t_0=\ln(\tilde{T}_{c0}/T_{cs})$, $t_t=\ln(\tilde{T}_{ct}/T_{cs})$, $\delta t_t=\ln(T_{cs}/T_{ct})$, and $\delta t_0=\ln(T_{cs}/T_{c0})$. Assuming $\Delta_0=0$, t_t is found to satisfy

$$t_t=-\delta t_t/\zeta_t\ , \tag{43a}$$

where

$$\zeta_t=1-\beta_{st}/\beta_s\ , \tag{43b}$$

provided that $\beta_s>\beta_{st}$. For $\beta_s\leq\beta_{st}$, $\tilde{T}_{ct}=0$. We note that, for $\beta_s\gg\beta_{st}$, $\tilde{T}_{ct}\approx T_{ct}$.

On the other hand, if we assume $\boldsymbol{\Delta}_t=0$, t_0 satisfies

$$t_0=-\delta t_0/\zeta_0\ , \tag{44a}$$

where

$$\zeta_0=1-b_0/(2\beta_s)\ . \tag{44b}$$

Comparing Eqs. (43) and (44), we see that, for $\beta_{st}<b_0/2$, the relative suppression $\tilde{T}_{c0}/T_{c0}$ is greater than that of $\tilde{T}_{ct}/T_{ct}$. More precisely, the ST phase is stable below $\tilde{T}_{ct}$, provided that $\tilde{T}_{ct}>\tilde{T}_{c0}$, which implies

$$T_{ct}/T_{cs}>(T_{c0}/T_{cs})^{\kappa}\ , \tag{45a}$$

where

$$\kappa=\zeta_t/\zeta_0\ . \tag{45b}$$

For $\tilde{T}_{c0}>\tilde{T}_{ct}$, the SS phase is stable below $\tilde{T}_{c0}$.

We first assume Eq. (45) is satisfied. Then the S phase is stable for $\tilde{T}_{ct}\leq T<T_{cs}$, and the ST phase for $T<\tilde{T}_{ct}$. In the ST phase ($t-t_t<0$), we have $|\Delta_0|=0$,

$$|\Delta_s|^2=-t/(2\beta_s)+(t-t_t)\zeta/(2\beta_s) \tag{46a}$$

and

$$|\Delta_t|^2=-\zeta(t-t_t)/(2\beta_{st}) , \tag{46b}$$

where

$$\zeta=\frac{\zeta_t}{\beta_t/\beta_{st}-\beta_{st}/\beta_s} , \tag{46c}$$

where t_t, ζ_t are given by Eq. (43). There is a second-order phase transition from the S to the ST phases at $\tilde{T}_{ct}$, provided that $\beta_s,\beta_t>\beta_{st}$. The anisotropy of the gap $2|\Delta(k_z,T)|$ is T dependent,

$$|\Delta(k_z,T)|^2=|\Delta_s|^2\langle u_{31}^{+}(k_z)|u_{31}^{+}(k_z)\rangle + |\Delta_t|^2\langle u_{31}^{-}(k_z)|u_{31}^{-}(k_z)\rangle , \tag{47}$$

where $|\Delta_s|^2$ and $|\Delta_t|^2$ are given in the S and ST phases by Eqs. (42) and (46). This gap is the same on both bands.

We now assume Eq. (45) is not satisfied $[T_{ct}/T_{cs}>(T_{c0}/T_{cs})^{\kappa}]$, so that the S phase is stable for $\tilde{T}_{c0}\le T>T_{cs}$, and the SS phase is stable for $T<\tilde{T}_{c0}$. In the SS phase, we have $t-t_0<0$ and $|\Delta_t|=0$,

$$|\Delta_0|^2=-(t-t_0)/b_0 \tag{48a}$$

and

$$|\Delta_s|^2=-t_0/(2\beta_s) , \tag{48b}$$

where t_0 is given by Eq. (44a). The transition from the S to the SS phase at $\tilde{T}_{c0}$ is second order. The gap $2|\Delta(k_z,T)|$ is the same on both bands, and nodeless at low T,

$$|\Delta(k_z,T)|^2=|\Delta_0|^2+|\Delta_s|^2\langle u_{31}^{+}(k_z)|u_{31}^{+}(k_z)\rangle . \tag{49}$$

In the S and SS' phases, $|\Delta_0|$ and $|\Delta_s|$ are given by Eqs. (42) and (48), respectively.

In order to investigate the possible existence of an additional phase with $|\Delta_s|$, $|\Delta_t|$, and $|\Delta_0|$, all simultaneously nonvanishing, we then choose the phases of Δ_0 and Δ_t to minimize their repulsive interactions with Δ_s. For these phase choices (Δ_0 and Δ_s out of phase by $\pi/2$, and Δ_t and Δ_s in phase), the repulsive interaction between Δ_t and Δ_0 is *maximized*. While we have not been able to rigorously prove that either $\tilde{T}_{c0}$ or $\tilde{T}_{ct}$ is always forced to zero, we have made numerous attempts to find regions in which all three OP's could be nonvanishing, but have been unsuccessful. Hence, we conclude on numerical grounds that, at most, two OP's can be simultaneously nonvanishing.

We note that, for both allowed cases of any two of the OP's, Δ_0, Δ_s, or Δ_t nonvanishing, the actual gap is twice the square root of the sum of the square magnitudes of the nonvanishing OP's times their respective normalized gap functions. For the Δ_s, Δ_t, combination, this arises because of the different matrix structure of those quantities in the Green's function. For the Δ_0, Δ_s combination, Δ_0 and Δ_s have similar (for $N=2$) and identical (for $N=1$) Green's-function matrix structure. However, the free energy is minimized when Δ_0 and Δ_s are $\pi/2$ out of phase. Hence, the above prescription for the gap is correct for both $N=1,2$.

In Figs. 4 and 5, we assume $\tilde{T}_{ct}>\tilde{T}_{c0}$, so that Δ_0 can be neglected. In Fig. 4, we have plotted the regions of different gap behavior in the parameter space. In the lower (upper) half of the figure, the regions are plotted for $0\le\lambda_1/\lambda_2\le 1$ ($1\ge\lambda_2/\lambda_1\ge 0$) and $0\le J_1/J_2\le 1$. Values for $1\ge J_2/J_1\ge 0$ are obtained by interchanging J_1 with J_2 and λ_1 with λ_2. Curve (a) separates region I, for which the dominant singlet gap function $|u_{31}^{+}(k_z)\rangle$ is nodeless, from region II, in which it has a pair of nodes. Curves (b), (c), and (d) correspond, respectively, to $|\Delta_t|=0.01|\Delta_s|$ at $T=0$ for the dimensionless eigenvalues $\lambda_{31}^{+}N(0)=0.2$, 1.0, and 2.0. These values are appropriate

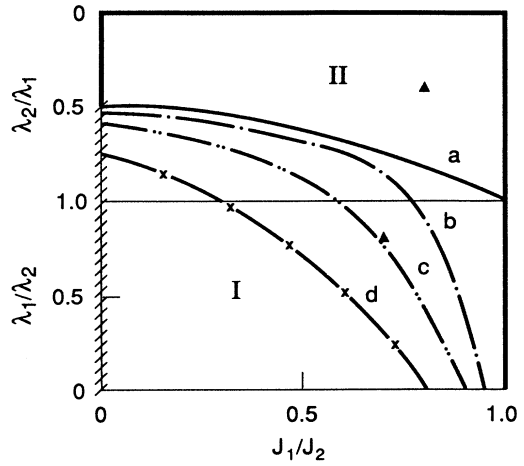

FIG. 4. Regions of different gap $2|\Delta|$ behavior for $N=2$ are shown for $0\le\lambda_1/\lambda_2\le 1$, $1\ge\lambda_2/\lambda_1\ge 0$, and $0\le J_1/J_2\le 1$. Regions for $1\ge J_2/J_1\ge 0$ are obtained from $J_1\leftrightarrow J_2$ and $\lambda_1\leftrightarrow\lambda_2$. On the dark exterior solid line, $T_{cs}=T_{ct}$, and Δ is isotropic. On the crosshatched line, Δ is isotropic and pure singlet. Curve (a) divides regions I and II, where the singlet gap function $|u_{31}^{+}(k_z)\rangle$ is nodeless or has a pair of nodes, respectively. Curves (b), (c), and (d) denote $|\Delta_t|=0.01|\Delta_s|$ at $T=0$ for $\lambda_{31}^{+}N(0)=0.2$, 1.0, and 2.0, respectively.

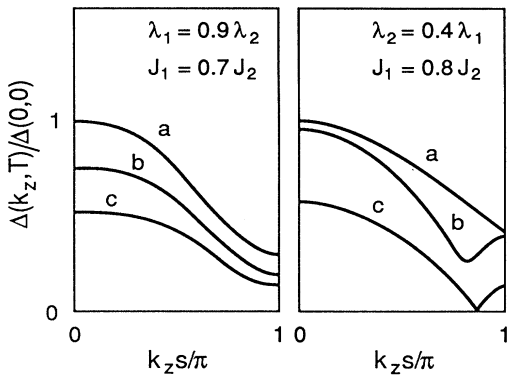

FIG. 5. Plots of $|\Delta(k_z,T)|/|\Delta(0,0)|$ vs k_zs/π for T/T_{cs} values of 0, 0.6, and 0.9 in curves (a), (b), and (c), respectively. Left plot: $\lambda_1/\lambda_2=0.9$, $J_1/J_2=0.7$. Right plot: $\lambda_2/\lambda_1=0.4$, $J_1/J_2=0.8$.

for weak, intermediate, and strong couplings, respectively. Below these curves, Δ_t (and the ST phase) can be neglected. Since region II is above all of these curves, we see that the gap is *always* nodeless at low T, even for weak-coupling strengths. Above the respective coupling strength curve, there will be two phases. Above these curves in region I, the gap is nodeless in both the S and ST phases. In region II, the gap has a node in the S phase (near to T_{cs}), but is nodeless in the ST phase (at lower T). In region II, the gap is nodeless for all $T<T_{cs}$.

In Fig. 5, we have plotted the gap $2|\Delta(k_z,T)|$, normalized by its $k_z=0$, $T=0$ value, as a function of $k_z s/\pi$, at three values of T/T_{cs}. In curves (a), (b), and (c), the T/T_{cs} values are 0, 0.6, and 0.9, respectively. In each case, we have used the weak-coupling limit $\lambda_{31}^{+}N(0)=0.2$. In the left figure, the parameters are $\lambda_1/\lambda_2=0.9$ and $J_1/J_2=0.7$, for which the normalized gap functions are plotted in the left figure in Fig. 3. This case corresponds to the triangle in region I of Fig. 4. Note that the gap is anisotropic, but the relative anisotropy is almost completely T independent, as $|\Delta_t|$ makes a relatively small contribution to $|\Delta|$ for all k_z values, even in the ST phase. In the right figure, $\lambda_2/\lambda_1=0.4$ and $J_1/J_2=0.8$. The normalized gap functions for this case were plotted in the right-hand figure in Fig. 3. This case corresponds to the triangle in region II of Fig. 4. Note that, at $T/T_{cs}=0.9$, which is in the S phase, the gap has a pair of nodes at $k_z s=\pm 0.86\pi$. However, in curve (b), $T/T_{cs}=0.6$, which in in the ST phase, the node has been removed. This T value is just below $\tilde{T}_{ct}$, so $|\Delta_t|\neq 0$, but $|\Delta_t|$ is still rather small. In curve (c), $T=0$, and $|\Delta_t|$ has increased substantially. The gap remains anisotropic, but all evidence of the node for $T>\tilde{T}_{ct}$ has been removed.

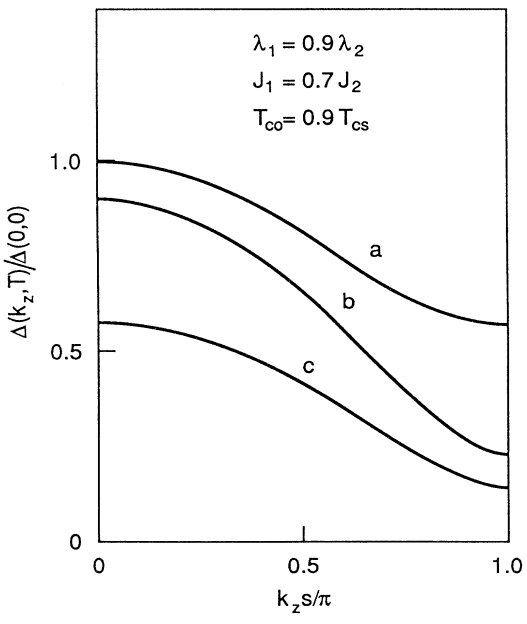

FIG. 6. Plotted is $|\Delta(k_z,T)|/|\Delta(0,0)|$ vs $k_z s/\pi$ for $\lambda_1/\lambda_2=0.9$, $J_1/J_2=0.7$, and $T_{c0}/T_{cs}=0.9$. Curves (a), (b), and (c) are for T/T_{cs} values 0, 0.5, and 0.9, respectively. In these curves, $\Delta_t=0$ and $\Delta_0\neq 0$ in curve (a).

In Fig. 6, we have plotted the gap $2|\Delta(k_z,T)|$ relative to its $k_z=0$, $T=0$ value, as a function of $k_z s/\pi$, for one case in which $|\Delta_0|$ and $|\Delta_s|$ are nonvanishing at low T. The parameters are $\lambda_1/\lambda_2=0.9$, $J_1/J_2=0.7$, and $T_{c0}/T_{cs}=0.9$, which correspond, for $\Delta_0=0$, to the left-hand figures in Figs. 3 and 5. The T/T_{cs} values chosen are (a) 0, (b) 0.5, and (c) 0.9. Although there are no nodes even just below T_{cs} for these parameters, the gap is highly anisotropic in the S phase near T_{cs}. At $T/T_{cs}=0.5$ (barely in the SS phase), the gap remains nearly as anisotropic as at $T/T_{cs}=0.9$, as $|\Delta_0|$ is small. However, at $T=0$ (well into the SS phase), $|\Delta_0|\neq 0$ greatly reduces the gap anisotropy.

VI. DISCUSSION

The model we have presented here has been solved in mean-field theory for the cases $N=1,2$. In our model, we have neglected the derivative of the density of states at the Fermi level, assuming $W_\perp/W_\parallel \ll 1$. Nonvanishing $W_\perp/W_\parallel$ leads to a term in the free energy δf_{30} in Eqs. (19) and (41) proportional to $(W_\perp/W_\parallel)\mathrm{Re}(\Delta_0^*\Delta_s)$. This term would cause Δ_s and Δ_0 to mix linearly, resulting in two solutions for the singlet transition temperature: the higher solution corresponds to a small amount of Δ_0 mixing with Δ_s. For $N=2$, this makes no essential difference. For $N=1$, there will then be two phases, as for $N=2$, and the gap would behave as in Eq. (47), where the singlet part contains a bit of Δ_0 mixing. For $W_\perp/W_\parallel \ll 1$, this correction will be small.

For $N=1$, $\hat{G}^{-1}$ has the SU(2)×SU(2) form, which can be written as a sum of products of two Pauli matrices. The Pauli matrices represent the spin and conventional Green's-function degrees of freedom, respectively. Both intralayer and interlayer pairing necessarily arise from the pairing of quasiparticles within the same band. For $N=2$, $\hat{\hat{G}}^{-1}$ has the SU(2)×SU(2)×SU(2) form, which can be represented in terms of three Pauli matrices. These Pauli matrices represent the spin, band, and conventional Green's function degrees of freedom, respectively. For general $N\geq 2$, there are N bands, each having a distinct k_z dispersion.[38] We would therefore expect $\hat{\hat{G}}^{-1}$ to have the SU(2)×SU(N)×SU(2) form, with an $N\times N$ matrix [the elements of which are the eigenstates of spin $(N-1)/2$] representing the band degrees of freedom. For SU(3), there are eight matrix generators[53] in addition to the identity matrix, two of which are traceless diagonal matrices of rank 3. These two diagonal matrices plus the identity matrix represent the intraband pairing gap functions. As shown elsewhere for $N=3,4$, the free energy has the form of Eq. (41), with different values for the various constants. The gaps on the different bands will not generally be equivalent, however.

We remark that Eq. (41) represents an accurate description of the GL free energy below the maximum T_c value. Above the maximum T_c, *all* of the gap functions with nonvanishing bare T_c values contribute to measur-

able quantities.[38] These extra contributions might account, in part, for the different effective mass ratio for the pairs inferred from fluctuation dimagnetism,[48] fluctuation conductivity,[54] magnetic torque,[24] and upper critical field[55] measurements. The Zeeman fluctuation conductivity fits[54] could be greatly altered. Fluctuation specific-heat fits[56] would be slightly modified, as the T range of the fits was limited.

Gap anisotropy between the c axis and the ab plane would certainly affect the apparent effective-mass anisotropy deduced from lower critical field[57] and magnetic penetration depth[1] experiments. It would also modify the interpretation of the NMR Knight shifts.[12] In a subsequent paper, we shall address those issues, most of which require introducing the magnetic vector potential for fields both along the c axis and in the ab plane.

The $N=1$ case is presumably appropriate for $La_{2-x}Sr_xCuO_4$ and may also be appropriate for the electron-doped materials $Nd_{2-x}Ce_xCuO_4$ and $Nd_{2-x}Th_xCuO_4$. The predicted lack of gap anisotropy for $N=1$ materials does not necessarily imply that the superconductors are conventional. One can obtain an isotropic gap either from the conventional s-wave intralayer BCS pairing, or from BCS-like interlayer pairing. In the latter case, the isotropic gap arises from an equal mixing of the singlet and triplet gap functions. We note that point-contact-tunneling experiments[15] on $La_{2-x}Sr_xCuO_4$ were interpreted as evidence for an isotropic gap. However, electron-spin-resonance experiments[58] on that material were interpreted as providing evidence for triplet hole pairs. Both conclusions would be consistent with interlayer pairing.

Doping experiments[59] are consistent with interlayer pairing in $La_{2-x}Sr_xCuO_4$ and Y 1:2:3 but with intralayer pairing in the $Nd_{2-x}Ce_xCuO_4$ system. In these experiments, a small amount of Cu is replaced with Ni, Co, or Zn. In $La_{2-x}Sr_xCuO_4$ and Y 1:2:3 nonmagnetic dopants (Zn) depress T_c as much as magnetic dopants. This is expected for interlayer pairing, especially[27] for $N=1$. In the $Nd_{2-x}Ce_xCuO_4$ system, doping with nonmagnetic ions was much less destructive to T_c than was doping with magnetic ions, as in a conventional superconductor.

For Y 1:2:3, it is likely that $N=2$. One possible contrary piece of evidence would be the Cu NMR experiments,[12] which indicated that the Cu-O chains have a Knight shift indicative of a gap distinct from the CuO_2 planes, which might be interpreted as giving $N=3$. However, this could possibly just be a manifestation of a k_z dependence of the overall gap. Infrared reflectance[4] and Raman-scattering[5] experiments suggest that the Cu-O chains may remain normal below T_c, which would also be a possible explanation for the linear term in the low-T specific heat consistently observed only in Y 1:2:3.[60] It is likely that the problem effectively separates into weakly coupled $N=2$ and (nearly normal) $N=1$ cases.

The Bi 2:2:1:2 material contains two CuO_2 layers and two Bi-O layers within a formula unit. Unlike the CuO_2 layers, the two Bi-O layers form one electronlike band at the Fermi level, both from band-structure calculations[20] and from photoemission experiments.[14] Hence, this is in reality an $N=3$ case. However, it is possible that the coupling between the predominantly Bi-O band to the predominantly CuO_2 bands is weak, reducing the problem to weakly coupled $N=2$ and 1 cases.

Finally, we would like to propose that a number of experiments be carried out to further elucidate the question of whether c-axis versus ab-plane gap anisotropy really does exist in Y 1:2:3 and possibly in other materials. One ought to look for evidence for a second phase transition, such as has recently been reported in specific-heat and magnetization studies on Y 1:2:3.[61] Angular-resolved photoemission experiments with a high degree of k_z resolution may prove useful. Repeated infrared reflectance and Raman-scattering measurements from the edge of single crystals is highly desirable. In addition, point-contact and Josephson tunneling into the ab-plane could be useful, especially in a magnetic field. To improve the interpretations of the data, more theory is needed to properly obtain the expected infrared reflectance and tunneling current results. One needs to take account of the normal-state layered structure and the gap anisotropy, and treat the rather clean limit for intralayer impurity scattering.

It would also be useful to perform experiments to investigate more thoroughly the electron-phonon mechanism. There is evidence of a possible local structural transition occurring at T_c in at least three materials,[5,46,47,62], which involves the different polarizations of the ionic motions differently. Hence, phonons and/or charge fluctuations are likely to be involved in the superconducting transition, and may be the driving force. If c-axis versus ab-plane gap anisotropy is indeed present for $N \geq 2$, it implies the appropriate pairing mechanism is likely to involve optical phonons propagating in the c-axis direction. Further neutron-scattering investigations of the polarizations and propagation directions of the phonons involved in this structural transition at T_c may prove useful. In particular, we suggest looking at the c-axis zone boundary for high-energy optical phonons.

ACKNOWLEDGMENTS

This work was supported by the U.S. Department of Energy, Division of Basic Energy Research, under Contract No. DE-AC05-84OR21400 with Martin Marietta Energy Systems, Inc., and under Contract No. W-31-109-ENG-38. Part of this work was performed while one of the authors (R.A.K) was at the Ames Laboratory, which is operated for the U.S. Department of Energy by Iowa State University under Contract No. W-7405-ENG-82.

APPENDIX

In this appendix, we obtain the determinants of the Green's functions for $N=1,2$. For future reference, we keep the Zeeman energy splitting $I=g\mu_B B/2$, where B is the magnetic induction.

For $N=1$, the mean-field equations for the elements $G_{\alpha\beta}$ and $F^{\dagger}_{\alpha\beta}$ are found to be

$$\{[i\omega-\xi_0(\mathbf{k})-2J_2\cos k_z s]\sigma_0+I\sigma_3\}\hat{G}-(\hat{\Delta}_3+\Delta_0\sigma_2)\hat{F}^\dagger=\sigma_0 \tag{A1a}$$

and

$$\{[i\omega+\xi_0(\mathbf{k})+2J_2\cos k_z s]\sigma_0-I\sigma_3\}\hat{F}^\dagger-(\hat{\Delta}_3^*+\Delta_0^*\sigma_2)\hat{G}=0\ , \tag{A1b}$$

where

$$\hat{\Delta}_3=\sum_{j=0}^{3}\Delta_{3j}\sigma_j\ , \tag{A2a}$$

$$\hat{G}=\sum_{j=0}^{3}G_j\sigma_j\ , \tag{A2b}$$

and

$$\hat{F}^\dagger=\sum_{j=0}^{3}F_j^\dagger\sigma_j\ , \tag{A2c}$$

where the σ_j are the Pauli spin matrices. We note that Eq. (A1) comprises eight equations from the Pauli matrix structure. We then combine those equations to obtain equations for $G_0\pm G_3$, $G_1\pm iG_2$, $F_0^\dagger\pm F_3^\dagger$, and $F_1^\dagger\pm iF_2^\dagger$. This effectively diagonalizes $\hat{G}$ and $\hat{F}^\dagger$ into 2×2 blocks. After some algebra, we obtain

$$\det(\hat{G})=D\prod_{S=\pm}\prod_{n=1}^{2}d_{nS}\ , \tag{A3a}$$

where

$$D=1+\sum_{S=\pm}(|\tilde{\Delta}_{30S}|^2/d_{1S}+|\tilde{\Delta}_{31S}|^2/d_{2S})+|\tilde{\Delta}_3^2|^2/(d_{1+}d_{1-})\ , \tag{A3b}$$

$$d_{1S}=\omega^2+[\xi_0(\mathbf{k})+2J_2\cos k_z s-SI]^2\ , \tag{A3c}$$

$$d_{2S}=(\omega-iSI)^2+[\xi_0(\mathbf{k})+2J_2\cos k_z s]^2\ , \tag{A3d}$$

$$\tilde{\Delta}_3(k_z)\equiv(i\Delta_{30}(k_z),\Delta_{31}(k_z),\Delta_{32}(k_z),\Delta_{33}(k_z))\ , \tag{A3e}$$

$$\tilde{\Delta}_{30S}=\tilde{\Delta}_{30}+iS\tilde{\Delta}_{33}\ , \tag{A3f}$$

$$\tilde{\Delta}_{31S}=\tilde{\Delta}_{31}+iS(\tilde{\Delta}_{32}+\Delta_0)\ . \tag{A3g}$$

All four-vector products are defined to be standard four-vector scalar products,

$$\tilde{\Delta}_i^2\equiv\sum_{j=0}^{3}(\tilde{\Delta}_{ij})^2 \tag{A4a}$$

and

$$|\tilde{\Delta}_i|^2\equiv\sum_{j=0}^{3}|\tilde{\Delta}_{ij}|^2\ . \tag{A4b}$$

The gap-function equations for Δ_0 and $\tilde{\Delta}_{3j}$ [Eq. (7) of the text] are then obtained from

$$\mathrm{Tr}[(\rho_1-i\rho_2)\sigma_j\hat{G}(k',\omega)]=-2\partial\ln\det(\hat{G})/\partial\tilde{\Delta}_{3j}^*(k_z')\ , \tag{A5}$$

etc., and integrating over $\xi_0(\mathbf{k}')$. This leads for $I=0$ to

$$\Delta_0=\tfrac{1}{4}N(0)sT\lambda_0\sum_{|\omega|\le\omega_\parallel}\sum_{S=\pm}\int_{-\pi/s}^{\pi/s}dk_z'\left[\frac{\Delta_0+\tilde{\Delta}_{32}+S(\delta R_{30}/\delta\Delta_0^*)}{(\omega^2+|\tilde{\Delta}_{3+0}|^2+SR_{30})^{1/2}}\right] \tag{A6a}$$

and

$$\tilde{\Delta}_{3j}(k_z)=\tfrac{1}{4}N(0)Ts\sum_{|\omega|\le\omega_\perp}\sum_{S=\pm}\int_{-\pi/s}^{\pi/s}dk_z'V(k_z,k_z')\left[\frac{\tilde{\Delta}_{3j}+\Delta_0\delta_{j2}+S(\delta R_{30}/\delta\tilde{\Delta}_{3j}^*)}{(\omega^2+|\tilde{\Delta}_{3+0}|^2+SR_{30})^{1/2}}\right]\ , \tag{A6b}$$

where

$$R_{30}^2=(|\tilde{\Delta}_{3+0}|^2)^2-|\tilde{\Delta}_{3+0}^2|^2 \tag{A6c}$$

and

$$\tilde{\Delta}_{3+0,j}(k_z)=\tilde{\Delta}_{3j}(k_z)+\delta_{j2}\Delta_0\ . \tag{A6d}$$

For $N=2$, the mean-field equations for the Green's-function matrix elements $\tilde{G}_{SS'}^{\alpha\beta}$ and $\tilde{F}_{SS'}^{\alpha\beta\dagger}$ are found to be

$$\{[i\omega-\xi_0(\mathbf{k})-S\varepsilon_\perp(k_z)]\sigma_0+I\sigma_3\}\hat{\tilde{G}}_{SS'}-S[(\hat{\Delta}_3+S\Delta_0\sigma_2)\hat{\tilde{F}}_{SS'}^\dagger-i(\hat{\Delta}_2+S\Delta_1\sigma_2)\hat{\tilde{F}}_{-S,S'}^\dagger]=\delta_{SS'}\sigma_0 \tag{A7a}$$

and

$$\{[i\omega+\xi_0(\mathbf{k})+S\varepsilon_\perp(k_z)]\sigma_0-I\sigma_3\}\hat{\tilde{F}}_{SS'}^\dagger-S[(\hat{\Delta}_3^*+S\Delta_0^*\sigma_2)\tilde{G}_{SS'}+i(\hat{\Delta}_2^*+S\Delta_1^*\sigma_2)\tilde{G}_{-S,S'}]=0\ , \tag{A7b}$$

where S, $S'=\pm$ are the band indices. As for $N=1$, we expand the matrices in Eq. (A7) in terms of the Pauli spin matrices,

$$\hat{\Delta}_i=\sum_{j=0}^{3}\Delta_{ij}\sigma_j\ , \tag{A8a}$$

for $i=2,3$,

$$\hat{\tilde{G}}_{SS'}=\sum_{j=0}^{3}\tilde{G}_{SS'j}\sigma_j \tag{A8b}$$

and

$$\hat{\tilde{F}}^{\dagger}_{SS'}=\sum_{j=0}^{3}\tilde{F}^{\dagger}_{SS'j}\sigma_j\ . \tag{A8c}$$

The eight resulting equations in the variables $\tilde{G}_{SS'0}\pm\tilde{G}_{SS'3}$, $\tilde{G}_{SS'1}\pm i\tilde{G}_{SS'2}$, $\tilde{F}^{\dagger}_{SS'0}\pm\tilde{F}^{\dagger}_{SS'3}$, and $\tilde{F}^{\dagger}_{SS'1}\pm i\tilde{F}^{\dagger}_{SS'2}$ can be combined to give four equations in the variables $\tilde{F}^{\dagger}_{SS'0}+\tilde{F}^{\dagger}_{SS'3}$, $\tilde{F}^{\dagger}_{-S,S'0}+\tilde{F}^{\dagger}_{-S,S'3}$, $\tilde{F}^{\dagger}_{SS'1}+i\tilde{F}^{\dagger}_{SS'2}$, and $\tilde{F}^{\dagger}_{-S,S'1}+i\tilde{F}^{\dagger}_{-S,S'2}$. After some algebra, the determinant of $\hat{\tilde{G}}$ is found to be

$$\det(\hat{\tilde{G}})=D\prod_{S,S'=\pm}\prod_{n=1}^{4}d_{nSS'}\ , \tag{A9a}$$

where

$$d_{1SS'}=\omega^2+[\xi_0(\mathbf{k})+S\varepsilon_{\perp}(k_z)-S'I]^2\ , \tag{A9b}$$

$$d_{2SS'}=(\omega+iS'I)^2+[\xi_0(\mathbf{k})+S\varepsilon_{\perp}(k_z)]^2\ , \tag{A9c}$$

$$d_{3SS'}=[\omega-iS\varepsilon_{\perp}(k_z)]^2+[\xi_0(\mathbf{k})-S'I]^2\ , \tag{A9d}$$

$$d_{4SS'}=[\omega-iS\varepsilon_{\perp}(k_z)+iS'I]^2+\xi_0^2(\mathbf{k})\ , \tag{A9e}$$

and

$$D=\begin{vmatrix} A_{++} & B_{++} & C_{++} & D_{++} \\ B_{-+} & A_{-+} & D_{-+} & C_{-+} \\ C_{+-} & D_{+-} & A_{+-} & B_{+-} \\ D_{--} & C_{--} & B_{--} & A_{--} \end{vmatrix}\ , \tag{A9f}$$

where

$$A_{SS'}=1+|\tilde{\Delta}_{30S'}|^2/d_{1SS'}+|\tilde{\Delta}_{31SS'}|^2/d_{2SS'}+|\tilde{\Delta}_{20S'}|^2/d_{3SS'}+|\tilde{\Delta}_{21SS'}|^2/d_{4SS'}\ , \tag{A9g}$$

$$B_{SS'}=-(\tilde{\Delta}^{*}_{30S'}\tilde{\Delta}_{20S'}/d_{1SS'}+\tilde{\Delta}^{*}_{21SS'}\tilde{\Delta}_{31SS'}/d_{2SS'}+\tilde{\Delta}^{*}_{20S'}\Delta_{30S'}/d_{3SS'}+\tilde{\Delta}^{*}_{31SS'}\tilde{\Delta}_{21SS'}/d_{4SS'})\ , \tag{A9h}$$

$$C_{SS'}=i(\tilde{\Delta}^{*}_{30S'}\tilde{\Delta}_{31S,-S'}/d_{1SS'}-\tilde{\Delta}^{*}_{31SS'}\tilde{\Delta}_{30,-S'}/d_{2SS'}+\tilde{\Delta}^{*}_{20S'}\tilde{\Delta}_{21S,-S'}/d_{3SS'}-\tilde{\Delta}^{*}_{21SS'}\tilde{\Delta}_{20,-S'}/d_{4SS'})\ , \tag{A9i}$$

$$D_{SS'}=-i(\tilde{\Delta}^{*}_{30S'}\tilde{\Delta}_{21S,-S'}/d_{1SS'}-\tilde{\Delta}^{*}_{31SS'}\tilde{\Delta}_{20,-S'}/d_{2SS'}+\tilde{\Delta}^{*}_{20S'}\tilde{\Delta}_{31S,-S'}/d_{3SS'}-\tilde{\Delta}^{*}_{21SS'}\tilde{\Delta}_{30,-S'}/d_{4SS'})\ , \tag{A9j}$$

$$\tilde{\Delta}_{30S'}=\tilde{\Delta}_{30}+iS'\tilde{\Delta}_{33}\ , \tag{A9k}$$

$$\tilde{\Delta}_{20S'}=\tilde{\Delta}_{20}+iS'\tilde{\Delta}_{23}\ , \tag{A9l}$$

$$\tilde{\Delta}_{31SS'}=\tilde{\Delta}_{31}+iS'(\tilde{\Delta}_{32}+S\tilde{\Delta}_0)\ , \tag{A9m}$$

$$\tilde{\Delta}_{21SS'}=\Delta_{21}+iS'(\tilde{\Delta}_{22}+iS\Delta_1)\ , \tag{A9n}$$

and

$$\tilde{\Delta}_2(k_z)=i(i\Delta_{20}(k_z),\Delta_{21}(k_z),\Delta_{22}(k_z),\Delta_{23}(k_z))\ . \tag{A9o}$$

For intralayer pairing alone, the resulting gap-function equations are

$$\Delta_0=\lambda_0 N(0)sT\sum_{|\omega|\le\omega_{\parallel}}\sum_{S=\pm}\int_{-\pi/s}^{\pi/s}\frac{dk_z'\Delta_0[\omega_S^2+|\Delta_0|^2+Z+\varepsilon_{\perp}^2(k_z')]-\Delta_0^{*}(\Delta_1)^2}{4Z[2(Z+X)]^{1/2}}\ , \tag{A10a}$$

and

$$\Delta_1=\lambda_0 N(0)sT\sum_{|\omega|\le\omega_{\parallel}}\sum_{S=\pm}\int_{-\pi/s}^{\pi/s}\frac{dk_z'\Delta_1[\omega_S^2+|\Delta_1|^2+Z-\varepsilon_{\perp}^2(k_z')]-\Delta_1^{*}(\Delta_0)^2}{4Z[2(Z+X)]^{1/2}}\ , \tag{A10b}$$

where $\omega_S=\omega-iSI$,

$$X=\omega_S^2+|\Delta_0|^2+|\Delta_1|^2-\varepsilon_{\perp}^2(k_z')\ , \tag{A10c}$$

$$Y^2=4\varepsilon_{\perp}^2(k_z')[\omega_S^2+|\Delta_0|^2)-4[\mathrm{Re}(\Delta_0^{*}\Delta_1)]^2\ , \tag{A10d}$$

and

$$Z=(X^2+Y^2)^{1/2}\ . \tag{A10e}$$

Expanding Eq. (A10) to order Δ_i^3 for $I=0$ leads to Eq. (25) of the text.

For $\Delta_1=\tilde{\Delta}_2=0$, the gap-function equations for $I=0$ reduce to

$$\Delta_0=\tfrac{1}{8}N(0)s\lambda_0 T\sum_{|\omega|\le\omega_{\parallel}}\sum_{SS'=\pm}\int_{-\pi/s}^{\pi/s}dk_z'\left[\frac{\Delta_0+S\tilde{\Delta}_{32}+S'(\delta R_{3S}/\delta\Delta_0^{*})}{(\omega^2+|\tilde{\Delta}_{3S}|^2+S'R_{3S})^{1/2}}\right] \tag{A11a}$$

and

$$\tilde{\Delta}_{3j}(k_z)=\frac{N(0)}{8}sT\sum_{|\omega|\le\omega_\perp}\sum_{SS'=\pm}\int_{-\pi/s}^{\pi/s}\tilde{V}'(k_z,k_z')dk_z'\left[\frac{\tilde{\Delta}_{3j}+S\Delta_0\delta_{j2}+S'(\delta R_{3S}/\delta\tilde{\Delta}_{3j}^*)}{(\omega^2+|\tilde{\Delta}_{3S}|^2+S'R_{3S})^{1/2}}\right], \tag{A11b}$$

where

$$R_{3S}^2=(|\tilde{\Delta}_{3S}|^2)^2-|\tilde{\Delta}_{3S}^2|^2 \tag{A11c}$$

and

$$\tilde{\Delta}_{3S}=(\tilde{\Delta}_{30},\tilde{\Delta}_{31},\tilde{\Delta}_{32}+S\Delta_0,\tilde{\Delta}_{33}) \tag{A11d}$$

is a four-vector obtained from $\tilde{\Delta}_3(k_z)$ by replacing $\tilde{\Delta}_{32}$ with $\tilde{\Delta}_{32}+S\Delta_0$.

For $\tilde{\Delta}_2$ or $\tilde{\Delta}_3$ alone, the gap-function equations for $I=0$ are

$$\tilde{\Delta}_i(k_z)=\tfrac{1}{8}N(0)Ts\sum_{|\omega|\le\omega_\perp}\int_{-\pi/s}^{\pi/s}dk_z'\tilde{V}'(k_z,k_z')\sum_{S,S'=\pm}\left[\frac{\tilde{\Delta}_i+S(\tilde{\Delta}_i|\tilde{\Delta}_i|^2-\tilde{\Delta}_i^*\tilde{\Delta}_i^2)/R_i}{(\omega_{iS'}^2+|\tilde{\Delta}_i|^2+SR_i)^{1/2}}\right] \tag{A12a}$$

for $i=2,3$, where

$$R_i^2=(|\tilde{\Delta}_i|^2)^2-|\tilde{\Delta}_i^2|^2\ , \tag{A12b}$$

$$\omega_{3S'}=\omega\ , \tag{A12c}$$

and

$$\omega_{2S'}=\omega-iS'\varepsilon_\perp(k_z')\ . \tag{A12d}$$

For interlayer pairing alone and $I=0$, the gap-function equations expanded to cubic order are found to be

$$\tilde{\Delta}_3(k_z)=\tfrac{1}{2}N(0)Ts\sum_{|\omega|\le\omega_\perp}\int_{-\pi/s}^{\pi/s}dk_z'\tilde{V}'(k_z,k_z')\left[\frac{\tilde{\Delta}_3}{|\omega|}-\{2\tilde{\Delta}_3|\tilde{\Delta}_3|^2-\tilde{\Delta}_3^*\tilde{\Delta}_3^2+2z_2[\tilde{\Delta}_3|\tilde{\Delta}_2|^2+\tilde{\Delta}_2(\tilde{\Delta}_2^*\tilde{\Delta}_3)-\tilde{\Delta}_2^*(\tilde{\Delta}_2\tilde{\Delta}_3)]+z_1[2\tilde{\Delta}_2(\tilde{\Delta}_2\tilde{\Delta}_3^*)-\tilde{\Delta}_3^*\tilde{\Delta}_2^2)\}/(2|\omega|^3)\right] \tag{A13a}$$

and

$$\tilde{\Delta}_2(k_z)=\tfrac{1}{2}N(0)Ts\sum_{|\omega|\le\omega_\perp}\int_{-\pi/s}^{\pi/s}dk_z'\tilde{V}'(k_z,k_z')\left[\frac{\tilde{\Delta}_2z_1}{|\omega|}-\{z_3[2\tilde{\Delta}_2|\tilde{\Delta}_2|^2-\tilde{\Delta}_2^*\tilde{\Delta}_2^2]+2z_2[\tilde{\Delta}_2|\tilde{\Delta}_3|^2+\tilde{\Delta}_3(\tilde{\Delta}_2\tilde{\Delta}_3^*)-\tilde{\Delta}_3^*(\tilde{\Delta}_2\tilde{\Delta}_3)]+z_1[2\tilde{\Delta}_3(\tilde{\Delta}_2^*\tilde{\Delta}_3)-\tilde{\Delta}_2^*\tilde{\Delta}_3^2]\}/(2|\omega|^3)\right], \tag{A13b}$$

where the $z_i(k_z')$ are identical to those given in Eq. (25) of the text.

As discussed previously, the gap-function equations are obtained by taking the logarithmic derivatives with respect to the complex conjugates of the appropriate gap functions. It is clear from Eq. (A9) that there are two types of pair breaking present here: Pauli pair breaking, arising from the Zeeman energy splitting of the nonparallel spin states, and interband pair breaking, for paired quasiparticles in different bands. Note that, for $\varepsilon_\perp, I \ll \max(\xi_0)$, $d_{1SS'}$ can be rewritten with an appropriate shift in ξ_0, removing both types of pair breaking. Pair breaking arises from the shifts in the Matsubara frequencies by $\pm iI$ or $\pm i\varepsilon_\perp$, respectively. All of the Δ_{2j} functions exhibit interband pair breaking, but the Δ_{3j} do not. In addition, the Δ_{i1} and Δ_{i2} functions exhibit Pauli pair breaking for both $i=2,3$, but the Δ_{i0} and Δ_{i3} functions do not.

The eigenfunctions and eigenvalues present in $\tilde{\Delta}_2$ and $\tilde{\Delta}_3$ are found in Sec. IV of the text, with the exception of the triplet $|u_{2n}^+(k_z)\rangle$ eigenfunctions and their corresponding eigenvalues $\alpha_{2n}^+(T)$, explicit forms for which were omitted from the text for brevity. These quantities are listed in the following.

Using Eq. (37b) in Eq. (28b) of the text, we first make a rotation through the angle θ_2 given by

$$\tan 2\theta_2=\frac{-2K_{12}^+(T)}{\alpha_-(T)}\ , \tag{A14a}$$

where

$$\alpha_\pm(T)=a_{21}^+(T)\pm a_{22}^+(T) \tag{A14b}$$

and K_{12}^+ and $a_{2n}^+(T)$ are given by Eq. (38). The eigenvalues $\alpha_{2n}^+(T)$ and eigenfunctions $|u_{2n}^+(k_z)\rangle$ are then given by

$$\alpha_{2n}^+(T)=[\alpha_+(T)\pm\bar{Z}(T)]/2\ , \tag{A14c}$$

$$\bar{Z}(T)=[\alpha_-^2(T)+4K_{12}^{+2}(T)]^{1/2}\ , \tag{A14d}$$

$$|u_{2n}^{+}(k_z,T)\rangle = J_2[a_{2\pm}(T)+b_{2\pm}(T)\cos k_z s]/\varepsilon_\perp(k_z)\ , \tag{A14e}$$

where

$$a_{2\pm}(T)=[a_\pm c_\pm(T)\mp a_\mp c_\mp(T)]/\sqrt{2}\ , \tag{A14f}$$

$$b_{2\pm}(T)=[b_\pm c_\pm(T)\mp b_\mp c_\mp(T)]/\sqrt{2}\ , \tag{A14g}$$

and

$$c_\pm(T)=[1\pm\alpha_-(T)/\bar{Z}(T)]^{1/2}\ . \tag{A14h}$$

The triplet eigenvalues $\alpha_{2n}^{+}(T)$ appear in Eqs. (39) and (40b) of the text.

Next, we evaluate the GL free energy for $N=2$. While it is possible for $N=2$ to find the GL free energy with Δ_0, Δ_1, $\tilde{\Delta}_3$, and $\tilde{\Delta}_2$ simultaneously nonvanishing, the resulting general expressions are sufficiently complicated (as well as unlikely) that we prefer to address the simplest special cases first, as most of the important physics can be addressed in this manner. We shall first consider the case of purely intralayer pairing. Next, we shall consider the case of purely interlayer pairing, neglecting $\tilde{\Delta}_2$. We then consider the case of both $\tilde{\Delta}_3$ and $\tilde{\Delta}_2$ nonvanishing. Finally, we consider $\tilde{\Delta}_3$ and the intralayer OP Δ_0 both nonvanishing.

The case of purely intralayer pairing is treated easily by the standard techniques. The free energy $F_{S01}-F_N=\frac{1}{2}N(0)f_{01}$ is found to be

$$f_{01}=|\Delta_0|^2\ln(T/T_{c0})+|\Delta_1|^2[\ln(T/T_{c1}^0)+\delta\alpha_1(T)]+\tfrac{1}{2}b_0(|\Delta_0|^2+|\Delta_1|^2)^2$$
$$+\tfrac{1}{2}c'(|\Delta_0+\Delta_1|^2-|\Delta_0|^2-|\Delta_1|^2)^2-c|\Delta_0|^2|\Delta_1|^2-d|\Delta_1|^4\ , \tag{A15}$$

where T_{c0} and T_{c1}^0 are given by Eqs. (8b) and (26a), and

$$b_0=7\zeta(3)/[8(\pi T)^2]\ , \tag{A16a}$$

$$c'=b_0-\frac{1}{(\pi T)^2}\sum_{n=0}^{\infty}(2n+1)^{-1}[(2n+1)^{-2}-(h_{n+}h_{n-})^{-1}]\ , \tag{A16b}$$

$$c=\frac{1}{(\pi T)^2}\sum_{n=0}^{\infty}\sum_{S=\pm}(2n+1)[(2n+1)^{-4}+(2n+1)^{-2}(h_{nS}h_{n,-S})^{-1}-2(h_{nS}h_{n,-S}^3)^{-1}]\ , \tag{A16c}$$

$$d=c+\frac{1}{2(\pi T)^2}\sum_{n=0}^{\infty}\sum_{S=\pm}(2n+1)^3\{(2n+1)^{-6}+2[(2n+1)^4h_{nS}h_{n,-S}]^{-1}$$
$$-7[(2n+1)^2h_{nS}^3h_{n,-S}]^{-1}+3[h_{nS}^5h_{n,-S}]^{-1}+[h_{nS}h_{n,-S}]^{-3}\}\ , \tag{A16d}$$

$$\delta\alpha_1(T)=\int_{-\pi}^{\pi}\frac{dx}{2\pi}\mathrm{Re}\{\psi[1/2+ig(x,T)]-\psi[1/2+ig(x,T_{c1}^0)]\}\ , \tag{A16e}$$

where

$$h_{n\pm}=[(2n+1)^2+(J_1\pm J_2)^2/(\pi T)^2]^{1/2} \tag{A16f}$$

and $g(x,T)$ is given by Eq. (26b).

We note that $\delta\alpha_1(T_{c1}^0)=0$. Examination of Eq. (A15) reveals that f_{01} is minimized if Δ_0 and Δ_1 are $\pi/2$ out of phase with each other, as this choice causes the term with coefficient $c'>0$ to vanish. Below T_{c0}, the mean-field $\Delta_0\neq 0$. Assuming $\Delta_1\neq 0$ below $T_{c1}<T_{c1}^0$, we obtain

$$[c(T_{c1})/b_0(T_{c1})]\ln(T_{c1}/T_{c1}^0)+\delta\alpha_1(T_{c1})$$
$$=\{1-[c(T_{c1})/b_0(T_{c1})]\}\ln(T_{c1}^0/T_{c0})\ . \tag{A17a}$$

Expanding to leading order in $t_1=T_{c1}/T_{c1}^0-1$ and $t_0=T_{c1}^0/T_{c0}-1$, we find

$$t_1\approx t_0(\pi T_{c1}^0/J)^2/C'\ , \tag{A17b}$$

where $J^2=J_1^2+J_2^2$ and

$$C'=93\zeta(5)/[14\zeta(3)]-7\zeta(3)/2\approx 1.52\ .$$

Hence, even if T_{c1}^0 is very near to T_{c0} (which occurs for $J/T_{c0}\ll 1$), the pair-breaking effects upon Δ_1 arising from the nonvanishing Δ_0 are sufficient to drive T_{c1} to zero. In the unlikely case of completely decoupled layers ($J_1=J_2=0$), $T_{c1}^0=T_{c0}$, the free energy is minimized when $|\Delta_0|=|\Delta_1|$ below T_{c0}. Otherwise, Δ_1 can be neglected entirely below T_{c0}. In the fluctuation regime above T_{c0}, however, both OP's could contribute, their relative contribution depending upon their respective bare T_c values. This comprises the zero-field aspects of the microscopic basis for a phenomenological model[38] used to fit the fluctuation diamagnetism data[48] on alighted Y 1:2:3 powder.

We now consider the case of purely interlayer pairing for $N=2$. The singlet order parameters are defined to be $\Delta_{sn}=\Delta_{32n}$ and $\Delta_s'=\Delta_{221}$. The triplet vector order parameters $\boldsymbol{\Delta}_t$ and $\boldsymbol{\Delta}_{tn}'$ have components $\Delta_{t\pm}=(\Delta_{301}\pm i\Delta_{331})/\sqrt{2}$, $\Delta_{t0}=\Delta_{311}$, $\Delta_{tn\pm}'=(\Delta_{20n}\pm i\Delta_{23n})/\sqrt{2}$, and $\Delta_{tn0}'=\Delta_{21n}$. We then write

$$\boldsymbol{\Delta}_t=\sum_{m=+,0,-}\hat{\mathbf{e}}_m\Delta_{tm} \tag{A18a}$$

and

$$\Delta'_{tn}=\sum_{m=+,0,-}\hat{\mathbf{e}}_m\Delta'_{tnm}\ , \tag{A18b}$$

where the $\{\hat{\mathbf{e}}_m\}$ form an orthonormal vector set.

The parameters coupling the various OP's in the gap functions $\tilde{\Delta}_3$ and in $\tilde{\Delta}_2$ are defined to be

$$\beta_{snn'n''n'''}=\tfrac{1}{2}b_0J^{3++}_{nn'n''n'''}\ ,$$
$$\beta'_{snn'n''n'''}=\tfrac{1}{2}b_0J^{2++}_{nn'n''n'''}\ , \tag{A19a}$$

$$\beta_t=\tfrac{1}{2}b_0J^{3--}_{1111}\ ,\quad \beta'_t=\tfrac{1}{2}b_0J^{2--}_{1111}\ , \tag{A19b}$$

and

$$\beta_{stnn'}=\tfrac{1}{2}b_0J^{3+-}_{nn'11}\ ,\quad \beta'_{stnn'}=\tfrac{1}{2}b_0J^{2+-}_{nn'11}\ , \tag{A19c}$$

where

$$J^{iSS'}_{nn'n''n'''}=\int_{-\pi}^{\pi}\frac{dx}{2\pi}\langle u^S_{in}(x/s)|u^{S'}_{in'}(x/s)\rangle \times\langle u^{S'}_{in''}(x/s)|u^{S'}_{in'''}(x/s)\rangle\zeta_i(x/s) \tag{A20}$$

for $i=2,3$, with $\zeta_3(x/s)=1$ and $\zeta_2(x/s)=z_3(x/s)$, which is given in Eq. (25e). The most important of these coupling parameters have been evaluated analytically. We have

$$\beta_t=\tfrac{3}{4}b_0,\quad \beta_{st}=\beta_{st11}=\tfrac{1}{4}b_0(1+b^2_-/2)\ , \tag{A21a}$$

$$\beta_s=\beta_{s1111}=\tfrac{1}{4}b_0[3+b^2_--(3+\eta)b^4_-/(4\zeta)+2a^2_-b^2_-/\zeta]\ , \tag{A21b}$$

and

$$\beta_{s2}=\beta_{s1112}=\frac{b_0}{16}[6b_+b_-(3-8/\zeta)+b_+b^3_-(22/\zeta-1)+8b^2_-(\eta/2\zeta)^{1/2}(3-b^2_-)]\ , \tag{A21c}$$

where η, ζ, $b_\pm$, and $a_\pm$ are given in Eqs. (31)–(33). In addition, we have the parameters that couple the OP's in $\tilde{\Delta}_2$ to those in $\tilde{\Delta}_3$,

$$\mu^{SS'}_{inn'n''n'''}=\tfrac{1}{2}b_0\int_{-\pi}^{\pi}\frac{dx}{2\pi}\langle u^S_{3n}(x/s)|u^{S'}_{3n'}(x/s)\rangle \times\langle u^{S'}_{2n''}(x/s)|u^{S'}_{2n'''}(x/s)\rangle z_i(x/s)\ , \tag{A22a}$$

and

$$\nu_{inn'}=\tfrac{1}{2}b_0\int_{-\pi}^{\pi}\frac{dx}{2\pi}\langle u^+_{3n}(x/s)|u^+_{2n'}(x/s)\rangle \times\langle u^-_{31}(x/s)|u^-_{21}(x/s)\rangle z_i(x/s) \tag{A22b}$$

for $i=1,2$, where z_1 and z_2 are given in Eq. (25).

We first consider the case $\tilde{\Delta}_2=0$. The GL free energy can readily be found to fourth order in the OP's Δ_{sn} and $\mathbf{\Delta}_t$. Although its exact form is rather complicated, we shall analyze it in detail, as some of the terms are not very important. We first analyze the singlet OP's alone. There are two singlet OP's, $\Delta_{sn}\equiv\Delta_{32n}$, each of which could become nonvanishing in the absence of the others below its respective bare T_c value, T^+_{c3n}. Clearly, the dominant singlet OP is $\Delta_s\equiv\Delta_{s1}$, with the highest-$T_c$ value, $T^+_{c31}=T_{cs}$. The dominant singlet terms in the free energy $F^+_S-F_N=\frac{1}{2}N(0)f^+_3$ may then be written as

$$f^+_3=|\Delta_s|^2\ln(T/T_{cs})+\beta_s|\Delta_s|^4 +|\Delta_{s2}|^2\ln(T/T^+_{c32})+4\beta_{s2}|\Delta_s|^2\,\mathrm{Re}(\Delta^*_s\Delta_{s2}) +2\beta_{s22}[2|\Delta_s|^2|\Delta_{s2}|^2+\mathrm{Re}(\Delta^{*2}_s\Delta^2_{s2})]+\cdots\ , \tag{A23}$$

where $\beta_s>0$, $\beta_{s2}=\beta_{s1112}$, $\beta_{s22}=\beta_{s1122}>0$, and we have employed the obvious symmetries of $\beta_{snn'n''n'''}$ given in Eq. (A19) above.

Since β_{s2} is, in general, nonvanishing, that term couples Δ_{s2} it linearly to $\Delta^*_s|\Delta_s|^2$, allowing Δ_{s2} to become nonvanishing. Numerically, however, it turns out that Δ_{s2} makes, at best, a 1% correction to the gap at low T. This is due to the fact that the quadratic coupling (i.e., the β_{s22} term) of Δ_{s2} to Δ_s is strongly *repulsive*, preventing $|\Delta_{s2}|$ from ever becoming comparable to $|\Delta_s|$. In short, it is almost always a good approximation to neglect Δ_{s2} altogether.

Next, we consider the possibility of $\tilde{\Delta}_2$ and $\tilde{\Delta}_3$ simultaneously nonvanishing. We have evaluated the full expression for the free energy $\frac{1}{2}N(0)f_{32}$, but its most general form is too lengthy to present here. Since $T_{cs}>T_{ct}$, in general, and $T'^0_{cs}=T^{-0}_{c21}$ is the highest of the possible T^{S0}_{c2n} values, it suffices to consider the effect of nonvanishing Δ_s upon $\mathbf{\Delta}'_t$, the latter being constructed out of the Δ_{2j1} for $j\neq2$ as in Eqs. (12) and (13). We find,

$$f_{32}\approx|\Delta_s|^2\ln(T/T_{cs})+|\mathbf{\Delta}'_t|^2[\ln(T/T'^0_{cs})+\delta\alpha_s(T)]+\beta_s|\Delta_s|^4 +\beta'_s[2(|\mathbf{\Delta}'_t|^2)^2-\mathrm{Re}(\mathbf{\Delta}'^{*2}_t\mathbf{\Delta}'^2_t)]+4\mu^{++}_2|\Delta_s|^2|\mathbf{\Delta}'_t|^2-2\mu^{++}_1\,\mathrm{Re}(\Delta^{*2}_s\mathbf{\Delta}'^2_t)\ , \tag{A24}$$

where $\beta'_s=\beta'_{s1111}$ and $\mu^{\pm\pm}_i=\mu^{\pm\pm}_{i1111}$ for $i=1,2$, which are given in Eq. (A22). Minimization of f_{32} occurs when Δ_s and the components of $\mathbf{\Delta}'_t$ are all in phase, or π out of phase. We then minimize f_{32} with respect to the amplitudes $|\Delta_s|$ and $|\mathbf{\Delta}'_t|$. The analysis is then precisely analogous with that following Eq. (A15), leading to the conclusion that the nonvanishing $|\Delta_s|$ below T_{cs} is strongly pair breaking upon $|\mathbf{\Delta}'_t|$, driving its actual transition temperature T'_{cs} to zero. Numerically, we have determined that it is *always* safe to neglect $\mathbf{\Delta}'_t$ below T_{cs}. We note, however, that $\tilde{\Delta}_2$ could play a role in the Gaussian fluctuation regime *above* the highest-T_c value (T_{cs} or T_{c0}), provided that at least one of the $T^{S0}_{c2n}\neq0$.

*Present address.
[1]S. Mitra *et al.*, Phys. Rev. B **40**, 2674 (1989).
[2]U. Welp *et al.*, Physica C **161**, 1 (1989); W. K. Kwok *et al.*, Phys. Rev. Lett. **64**, 966 (1990).
[3]R. T. Collins *et al.*, Phys. Rev. Lett. **63**, 422 (1989).
[4]Z. Schlesinger *et al.*, Phys. Rev. Lett. **65**, 801 (1990).
[5]K. McCarty, Phys. Rev. B **42**, 9973 (1990); M. Boekholt, M. Hoffmann, and G. Güntherodt, Physica C **175**, 127 (1991).
[6]J. S. Tsai *et al.*, Physica C **157**, 537 (1989).
[7]M. Gurvitch *et al.*, Phys. Rev. Lett. **63**, 1008 (1989).
[8]G. Briceno and A. Zettl, Solid State Commun. **70**, 1055 (1989).
[9]L. H. Greene *et al.*, Physica C **162-164**, 1069 (1989); in *High Temperature Superconductors: Fundamental Properties and Novel Materials Processing,* edited by D. Christen, J. Narayan, and L. F. Schneemayer, MRS Symposia Proceedings (Materials Research Society, Pittsburgh, 1990), p. 991; H. Akoh *et al.*, Jpn. J. Appl. Phys. **27**, L519 (1988).
[10]M. R. Beasley *et al.* (unpublished).
[11]P. C. Hammel *et al.*, Phys. Rev. Lett. **63**, 1992 (1989); M. Takigawa *et al.*, *ibid.* **63**, 1865 (1989).
[12]C. Slichter *et al.*, Bull. Am. Phys. Soc. **35**, 276 (1990); C. H. Pennington *et al.*, Phys. Rev. B **39**, 2902 (1989); M. Takigawa *et al.*, Phys. Rev. B **39**, 7371 (1989).
[13]A. Arko *et al.*, Phys. Rev. B **40**, 2268 (1989); C. G. Olson *et al.*, Science **245**, 731 (1989).
[14]C. G. Olson *et al.*, Solid State Commun. **76**, 411 (1990); R. Manzke, T. Buslaps, R. Claessen, and J. Fink, Europhys. Lett. **9**, 477 (1989); A. Arko (private communication).
[15]L. N. Bulaevskii *et al.*, Supercond. Sci. Technol. **1**, 205 (1988).
[16]T. Ekino and J. Ekimitsu, Phys. Rev. B **40**, 7364 (1989); J. Tsai, T. Manako, and Y. Kubo, *ibid.* **40**, 9286 (1989).
[17]S. H. Wang *et al.*, Phys. Rev. Lett. **64**, 1067 (1990).
[18]J. Zasadzinski *et al.* (unpublished); (private communication).
[19]L. Smedskjaer *et al.*, Physica C **156**, 269 (1988).
[20]Z.-X. Shen *et al.*, Phys. Rev. B **38**, 7152 (1988); S. Massidda, J. Yu, and A. J. Freeman, Physica C **152**, 251 (1988).
[21]F. M. Mueller *et al.*, Bull. Am. Phys. Soc. **35**, 550 (1990); Physica B (to be published).
[22]S. W. Tozer *et al.*, Phys. Rev. Lett. **59**, 1768 (1987); S. Hagen *et al.*, Phys. Rev. B **37**, 7928 (1988); D. A. Brawner, Z. Z. Wang, and N. P. Ong, *ibid.* **40**, 9329 (1989).
[23]S. Martin *et al.*, Phys. Rev. Lett. **60**, 2194 (1988).
[24]D. E. Farrell *et al.*, Phys. Rev. Lett. **64**, 1573 (1990).
[25]R. A. Klemm and S. H. Liu, Physica C **176**, 189 (1991); S. H. Liu and R. A. Klemm, Chin. J. Phys. (Taiwan) **29**, 157 (1991).
[26]K. B. Efetov and A. I. Larkin, Zh. Eksp. Teor. Fiz. **68**, 155 (1975) [Sov. Phys. JETP **41**, 76 (1975)].
[27]R. A. Klemm and K. Scharnberg, Phys. Rev. B **24**, 6361 (1981).
[28]Zs. Gulácsi, M. Gulácsi, and I. Pop, Phys. Rev. B **37**, 2247 (1988).
[29]T. Schneider and D. Baeriswyl, Z. Phys. B **73**, 5 (1988).
[30]J. Ihm and B. D. Yu, Phys. Rev. B **39**, 4760 (1989).
[31]Y. Suwa, Y. Tanaka, and M. Tsukada, Phys. Rev. B **39**, 9113 (1989); Y. Suwa and M. Tsukada, *ibid.* **41**, 2113 (1990).
[32]T. Schneider, H. De Raedt, and M. Frick, Z. Phys. B **76**, 3 (1989).
[33]Z. Tešanović, Phys. Rev. B **36**, 2364 (1987); **38**, 2489 (1988).
[34]L. N. Bulaevskii and M. V. Zyskin, Phys. Rev. B **42**, 10230 (1990).
[35]J. Appel and D. Fay, Phys. Rev. B **41**, 873 (1990).
[36]S. S. Jha, Pramana J. Phys. **29**, L615 (1987); S. S. Jha, Rev. Solid State Sci. **2**, 307 (1988); S. S. Jha and A. K. Rajagopal, Physica C **168**, 173 (1990).
[37]J. Birman and J.-P. Lu, Phys. Rev. B **39**, 2238 (1989).
[38]R. A. Klemm, Phys. Rev. B **41**, 2073 (1990).
[39]Y. Shimakawa *et al.*, Phys. Rev. B **40**, 11400 (1989); Y. Kubo *et al.*, *ibid.* **43**, 7875 (1991).
[40]L. Pintchovius *et al.*, Phys. Rev. B **40**, 2229 (1989); R. J. Birgeneau *et al.*, Phys. Rev. Lett. **59**, 1329 (1987); P. Böni *et al.*, Phys. Rev. B **38**, 185 (1988); B. Renker *et al.*, Z. Phys. B **67**, 15 (1987).
[41]W. Reichardt *et al.*, Bull. Am. Phys. Soc. **35**, 782 (1990); (unpublished).
[42]W. Reichardt *et al.* (unpublished).
[43]M. K. Crawford *et al.*, Phys. Rev. B **41**, 282 (1990); Bull. Am. Phys. Soc. **36**, 387 (1991).
[44]J. P. Franck *et al.*, Physica C **162-164**, 753 (1989); E. Altendorf *et al.*, Phys. Rev. B **43**, 2771 (1991).
[45]S. Bhattacharya *et al.*, Phys. Rev. B **37**, 5901 (1988); Y. Horie, T. Fukama, and S. Mase, Solid State Commun. **63**, 653 (1987); M. J. Higgins *et al.*, Phys. Rev. B **40**, 9393 (1989).
[46]R. P. Sharma *et al.*, Phys. Rev. B **38**, 9287 (1988); T. Haga *et al.*, *ibid.* **41**, 826 (1990).
[47]H. Mook, Phys. Rev. Lett. **65**, 2712 (1990); Bull. Am. Phys. Soc. **36**, 387 (1991).
[48]W. C. Lee, R. A. Klemm, and D. C. Johnston, Phys. Rev. Lett. **63**, 1012 (1989).
[49]K. Maki, in *Superconductivity,* edited by R. D. Parks (Marcel Dekker, New York, 1969), p. 1035.
[50]A. Abrikosov, L. Gor'kov, and I. Dzyaloshinskii, *Methods of Quantum Field Theory in Statistical Physics* (Prentice-Hall, Englewood Cliffs, NJ, 1963).
[51]R. A. Klemm, A. Luther, and M. R. Beasley, Phys. Rev. B **12**, 877 (1975).
[52]L. N. Bulaevskii, Zh. Eksp. Teor. Fiz. **64**, 2241 (1973).
[53]M. Gell-Mann, in *The Eight-fold Way,* edited by M. Gell-Mann and Y. Ne'eman (Benjamin, New York, 1964), p. 49.
[54]A. G. Aronov, S. Hikami, and A. I. Larkin, Phys. Rev. Lett. **62**, 965 (1989).
[55]U. Welp *et al.*, Phys. Rev. Lett. **62**, 1908 (1989).
[56]S. E. Inderhees *et al.*, Phys. Rev. Lett. **60**, 1178 (1988); **66**, 232 (1991).
[57]A. Malozemoff *et al.*, Phys. Rev. B **38**, 7203 (1988).
[58]H. Thomann *et al.*, Phys. Rev. B **38**, 6552 (1988).
[59]J. M. Tarascon *et al.* (unpublished).
[60]R. A. Fisher, J. E. Gordon, and N. E. Phillips, J. Supercond. **1**, 231 (1988); S. E. Stupp and D. M. Ginsberg, Physica C **158**, 299 (1989).
[61]W. C. Lee *et al.*, Phys. Rev. B **43**, 463 (1991).
[62]B. H. Toby *et al.*, Phys. Rev. Lett. **64**, 2414 (1990).